Memoirs of the Faculty of Engineering, Nagoya University
Vol. 34, No. 2 (1982)

WAVE DEFORMATION IN THE SURF ZONE

KOICHIRO IWATA and TORU SAWARAGI*

Department of Civil Engineering

(Received October 29, 1982)

Abstract

An elucidation of mechanics of wave breaking and wave deformation after breaking has been a matter of great interest to coastal engineers as well as researchers in the hydrodynamics field.

This paper is intended to discuss the wave characteristics at the inception of wave breaking and the wave deformation in the surf zone up to the dry bed from theories and experiments. Waves treated in this paper are both the regular and irregular waves.

The wave breaking conditions and breaker types, wave characteristics such as the wave height, wave profiles, etc., at the breaking point, internal mechanics of breaking waves, changes of wave heights and the mean water levels, and wave run-up heights are described. Main part of the paper discusses the regular wave deformation in the surf zone.

CONTENTS

* Osaka University (formerly, Associate Professor, Department of Civil Engineering, Nagoya University)

1. Introduction

As a wave generated in deep water moves in shallow water area of which water depth is less than one-second times the wave length, the wave modifies its height and length due to shoaling, bottom friction, percolation, reflection, etc., and then the wave peaks up at crest and flattens at trough.

It is well known that a wave is transformed largely by current (e. g., tidal current), or by diffraction, reflection, etc., caused by coastal structures such as breakwaters. As the wave propagates in shallower water, the wave loses its symmetrical shape and becomes to show a steeper front face, and finally the wave breaks as the result of destruction of the wave motion. The breaking wave or the broken wave is finally transformed to a run-up wave or up-rush and back-rush in the swash zone.

The transformation process of wave breaking up to a current like the uprush and backrush in the surf and swash zones is strongly non-linear. Therefore, the clarification of the process has not been made in depth. Because of this, it may safely be said that the mechanics of sand movements is still an unexact science. Moreover, since most of coastal structures such as sea-dikes, off-shore breakwaters, and jetties being used as shore protection works have been constructed in the shallow water surf, it is necessary for the rational and economical design of the coastal structures to predict precisely the wave characteristics in the shallow water surf.

As mentioned above, since the prediction of wave transformation in the shallow

water surf is significantly important, many experimental and theoretical studies have been carried out. Investigations on waves in the surf are divided into two subjects, i. e., the mechanics of wave breaking and the process of wave deformation after breaking.

The study on the mechanics of wave breaking was first done experimentally by Iversen[1] in 1951. Since then, the wave breaking mechanics and breaker types have been investigated energetically from theories and experiments. It has been thought that each of breakers has its own wave breaking mechanics and then measurements of the water particle velocities have been performed in order to make clear the wave kinematics. However, the precise measurement of the water particle velocity at the wave breaking inception is extremely difficult due to the lack of highly accurate measuring instruments as well as the unstable phenomenon of wave breaking itself. Then, so far, the modeling of the wave breaking condition has been proposed to discuss wave characteristics such as the wave height, the wave steepness, etc., at the breaking point. And, by applying the proposed breaking conditions to finite amplitude wave theories in deep water and shallow water, solitary wave theories, cnoidal wave theories, and long wave theories, wave properties such as the wave height, wave steepness, etc., at the breaking point have been calculated theoretically and have been compared with experiments in order to show the propriety of the proposed wave breaking models. Concerning the regular wave, some characteristics of wave breaking mechanics have been made clear and they are applied for practical use. On the other hand, the history of investigations on the mechanics of irregular wave breaking is still young, and detailed and systematic researches are needed to elucidate the mechanics of irregular wave breaking.

The process of wave transformation after breaking up to the run-up/run-down wave in the surf zone is strongly non-linear with dissipation of a lot of wave energy, therefore the mathematical treatment is extremely difficult. However, speaking from the engineering point of view, the wave in the surf is usually very important physical factor giving the external force for the coastal and shore protection structures. Therefore, many theoretical and experimental investigations have been performed in order to establish a method to predict the wave deformation. Regarding to the regular wave, a lot of investigations have been carried out. Despite that, the basic equation describing the wave in the surf zone has not been successfully deduced, although many theoretical models have been proposed. Studies on the deformation of irregular wave in the surf have begun very recently, and some theoretical treatments have been presented. The quantitative agreement between the proposed theories and experiments, however, has not yet obtained. This is largely due to the reason that the mechanics of the depth-limitted wave breaking has not been clarified. Then, it is thought that systematic theoretical and experimental studies are needed to make clear the mechanics of wave transformation of the irregular wave.

In this paper, the breaking condition and criteria are described in chapter 2. In chapter, 3, breaker types are discussed for the regular and irregular waves. Chapter 4 describes wave chracteristics at the breaking point in relation to the breaker index. In chapter 5, the mechanics of wave breaking is dealt with in relation to the horizontal roller, bottom friction and turbulence caused by wave breaking. A theoretical method to predict the wave height changes is presented in chapter 6. Section 7 treats the wave run-up height, and the theoretical estimation method is presented.

2. Breaking conditions

Since the wave breaking is an extreme limit of the wave motion, many breaking conditions indicating the extreme limit for the wave motion have been presented in order to determine wave characteristics at the breaking point such as the breaking wave height H_b, the breaking wave length L_b, etc., from theoretical analyses. The following breaking conditions have been proposed.

Wave breaking occurs,

(1) when the particle velocity at wave crest becomes larger than the wave celerity,

(2) when the wave peaks up and the cusped crest shows the angle of 120°,

(3) when the wave profile loses a symmetrical shape and the wave front surface becomes vertical,

(4) when the difference between the particle velocity at wave crest and at bottom bed becomes extraordinary large and the wave crest moves much faster than the other portion of wave,

(5) when an equation expressing a wave loses its stationary solution, i. e. when infinite power series of finite amplitude wave diverge,

and,

(6) when the curves of characteristics describing the non-linear shallow water wave intersect each other and form an envelope curve.

Breaking criteria can be deduced by applying the above-mentioned breaking conditions to wave theories such as finite amplitude periodic wave theories in deep or shallow water depth, solitary wave theories, and finite amplitude long wave theories. So far, a number of breaking criteria have been published.

The breaking condition (1) mentioned above was first proposed by Rankine[2] and is very popular at present. Boussinesq[3], McCowan[4] and Munk[5] proposed breaking criteria for the solitary wave, and Miche[6], Hamada[7], Sato[8] and Kishi[9] presented breaking criteria for shallow water periodic waves. The breaking condition (2) was first defined by Stokes[10]. The condition (2) equals to the condition (1) in the case of McCowan's solitary wave theory. $H_b/L_b=0.142$ by Michell is well known as typical breaking limit for the deep water wave.

Based on the condition (3), Greenspan[11], Kishi[12], and Murota[13] deduced several breaking criteria for a long wave. The breaking point predicted by the theories, however, depends on an initial wave profile. This makes it difficult for the condition (3) to be applied to the actual breaker.

The breaking condition (4) can be applied in a breaking limit for waves in the near shore having a strong backwash or for waves advancing against or on a stream.

Shuto[14] developed a breaking criterion by use of the condition (5). Generally, it may be difficult to derive the breaking limit by use of condition (5).

Stoker[15] first presented the breaking condition (6). However, the condition (6) is not so useful in obtaining the breaking limit, because the breaking point depends largely on an initial wave profile as well as the starting point of calculation for the wave deformation, like condition (3).

It should be noted that all of the above-mentioned breaking criteria are proposed for waves which break in a constant water depth. Therefore, a number of em-

pirical breaking limit using results of laboratory experiments have been published for the wave which breaks on a sloping bed. The breaking criteria popular among above-cited theoretical and emperical expressions for both horizontal and sloping bottoms are;

McCowan's criterion;

$$H_b/h_b=0.78 \text{ (for solitary wave)}, \tag{1}$$

Mich's criterion;

$$H_b/L_b=0.142 \tanh 2\pi h_b/L_b \tag{2}$$

(for shallow water periodic wave),

Le Méhauté's[16] criterion (emperical criterion);

$$H_b/H_0=0.76(\tan\theta)^{1/7}(H_o/L_o)^{-1/4}, \tag{3}$$

Goda's[17] criterion;

$$H_b/L_o=A\left(1-\exp\left[-1.5\pi\frac{h_b}{L_o}(1+15\tan\theta^{4/3})\right]\right). \tag{4}$$

In Eqs. (1) ~ (4), $\tan\theta$ is the beach slope, h_b is the breaking water depth, L_o and H_o are respectively the wave length and height in deep water depth. A in Eq. (4) is a numerical constant of which value is from 0.12 to 0.18, and 0.17 is usually used.

3. Breaker types

3. 1. *Regular wave*

As already mentioned in previous sections, when a wave shoals in a certain water depth, the wave peaks up and then the wave front becomes steeper than the back face, and finally the wave breaks as its extreme limit for the wave motion. The broken wave with air-bubble at wave front propagates some distance towards the shoreline. The region where the broken wave advances is usually called the surf zone. Breaker types as limit forms of waves are classified into three types[18,*] as indicated in Fig. 1.

a) Spilling breaker: The limiting wave shape is not so unsymmetrical as the case of the plunging breaker. The spilling breaker is characterized by the appearance of "white water" at the crest; they break gradually. Bubbles and turbulent water spill down front face of wave.

b) Plunging breaker: The plunging breaker shows a very unsymmetrical profile with steeper front surface compared to the back surface. The crest curls over a large air pocket. Air-entrained horizontal roller and splash usually follows.

*) Galvin[19] defined the collapsing breaker as one breaker type and classified breakers into four types, i. e., the spilling breaker, plunging breaker, surging breaker and collapsing breaker. The collapsing breaker occurs over lower half of wave. Minimal air pocket and usually no splash-up. Bubbles and foam present.

c) Surging breaker: The wave peaks up as if to break in the manner of the plunging breaker, but when the base of the wave surges up the beach face with the resultant disappearance of the collapsing wave crest.

Iversen, and Hayami[20] pointed out that these breaker types can be classified by the wave steepness in deep water, H_o/L_o and the beach slope, $\tan\theta$. Recently, Battjes[21] showed that the surf similarity parameter ξ_b defined by Eq. (5) can classify the breaker types successfully as given by Eq. (6).

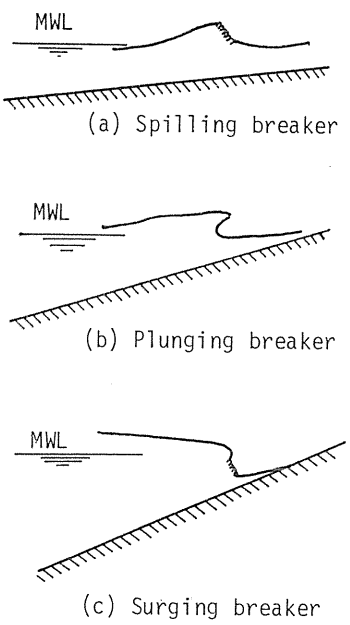

Fig. 1. Breaker types.

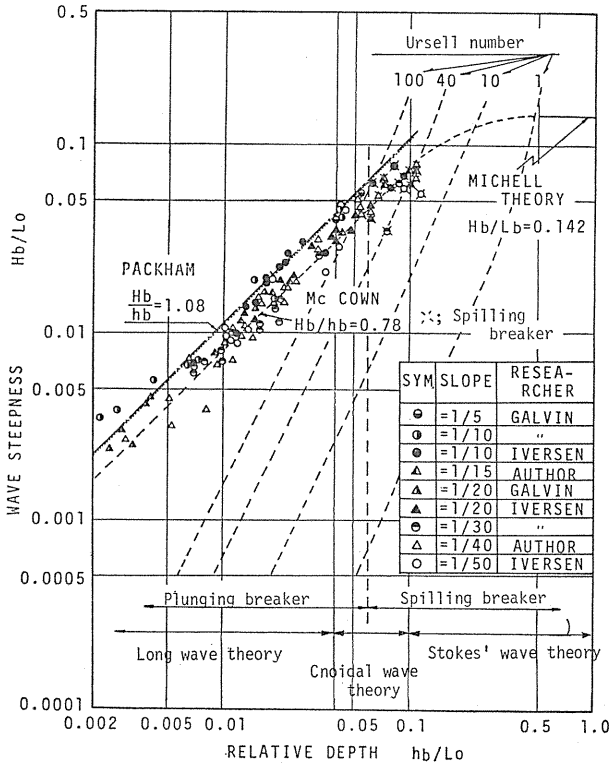

Fig. 2. Classification of breaker types due to shallowness.

$$\xi_b=\frac{\tan\theta}{\sqrt{H_b/L_o}}=\frac{1}{\sqrt{2\pi}}\frac{\tan\theta}{\sqrt{H_b/gT^2}}, \tag{5}$$

$$\left.\begin{aligned}&\text{surging breaker}: && \xi_b>2.0\\ &\text{plunging breaker}: && 0.4<\xi_b<2.0\\ &\text{spilling breaker}: && 0.4<\xi_b\end{aligned}\right\}. \tag{6}$$

The classification of breakers by the parameter of the wave steepness and the beach slope does not correspond well to hydrodynamic meaning. The present au-

thors[22] tried to classify breaker types by the parameters of H_b/L_o and h_b/L_o which were used by Wilson[23] in the classification of wave theories, and the authors examined the relation between breaker types and wave theories. Fig. 2 shows the result. The figure indicates that the Stoke's wave theory[24] is useful for describing the spilling breaker, the long wave theory for the plunging breaker, and the cnoidal or solitary wave theories for the transient state from the spilling breaker to the plunging breaker.

3. 2. *Irregular wave*

Discussions on breaker types of the irregular wave have not been done enough. The present authors[25] discussed the classification between the spilling and plunging breaker. Fig. 3 shows a relation between the surf similarity parameter ξ_b and two types of breakers, where L_o is the wave length in deep water calculated from L_b by the linear wave theory[24]. In the figure, symbols of ●, ▲ and ■ mean

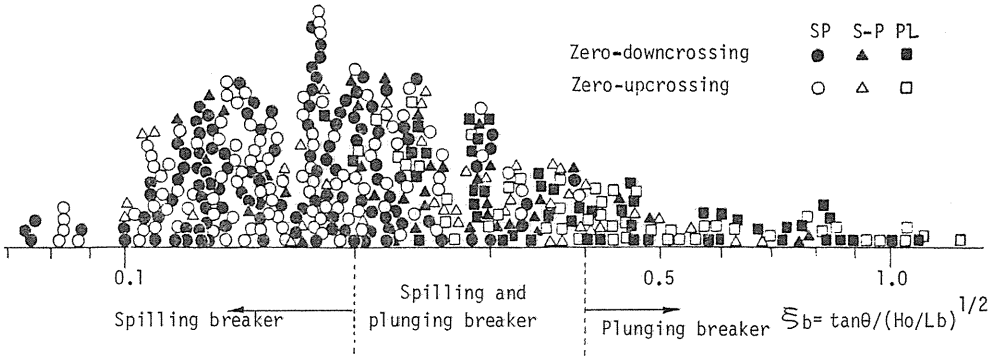

Fig. 3. Breaker type classification due to surf similarity parameter.

the zero-downcrossing wave and the symboles of ○, △ and □ mean the zero-upcrossing wave, *SP*, *PL*, and *S-P* indicate the spilling breaker, the plunging breaker, and the intermediate breaker, respectively. Judging from Fig. 3, it is seen that there is no significant difference between the zero-upcrossing and zero-downcrossing wave in classifing the breaker types. Breaker types can be roughly classified as follow,

$$\begin{aligned} &\text{spilling breaker :} && \xi_b \leq 0.2, \\ &\text{plunging breaker :} && \xi_b \geq 0.4, \\ &\text{intermediate breaker :} && 0.2 < \xi_b < 0.4. \end{aligned} \tag{7}$$

The surging or collapsing breaker should give an upper limit to the plunging breaker occurrence. However, the range where the surging or collapsing breaker takes place has not investigated. By the way, Eq. (7) is very similar to Eq. (6) for the regular wave. Weishar and Byrne[26] measured breaker types and waves at breaking points on the natural beach. Their classification of the plunging breaker almost coincides with our indoor experiments. But, the range of the occurrence

of the spilling breaker is very different from our result. They pointed out that the spilling breaker occurs independent of the surf similarity parameter. The difference may be largely caused by the difference of sea bottom configuration and the existence or non-exsistence of wind. For these points, further investigations will be needed to clarify the difference.

4. Wave properties at breaking point

4. 1. Regular wave

The breaking wave height and length given by Eqs. (1) through (4) are some of wave properties at breaking point. The wave height and length, and breaking water depth measured in laboratory tanks are, however, different among investigators, since the wave breaking is phenomenon which takes place in the extreme limit state.

Goda[27] re-analyzed many experimental data obtained from laboratory flumes by subtracting effects of side-wall and bottom friction, and he presented figures (Figs. 4, 5 and 6) which give wave characteristics at breaking point. The figures

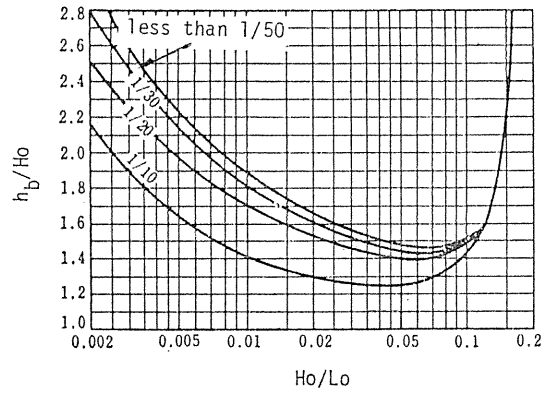

Fig. 4. Variation of breaking water depth (from Goda[27]).

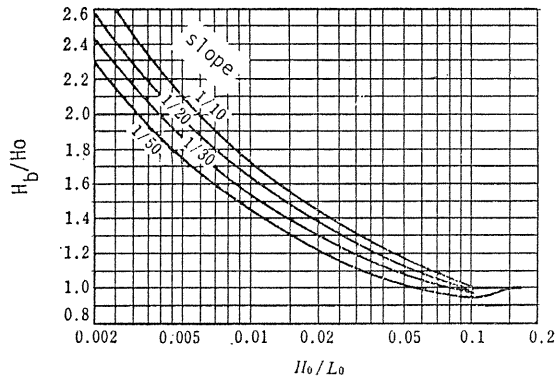

Fig. 5. Variation of breaking wave height (from Goda[27]).

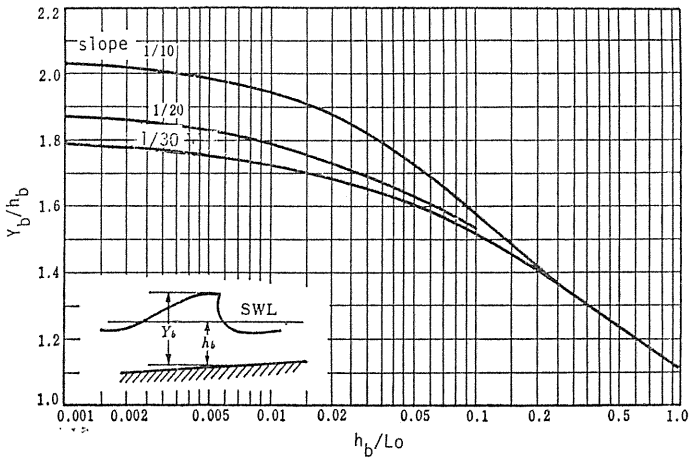

Fig. 6. Variation of breaking wave crest height (from Goda[27]).

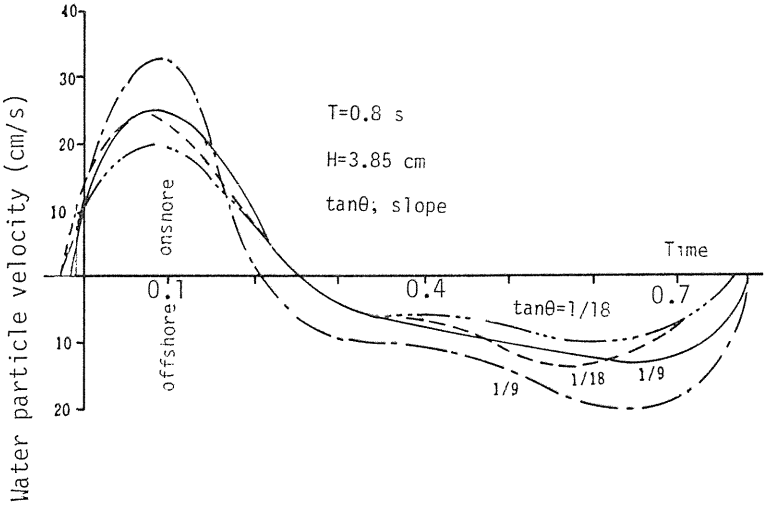

Fig. 7. Time profile of water particle velocity at breaking point (from Kemp[28]).

are called Breaker Index.

The field of the water particle velocity at breaking point and in the surf has not been revealed sufficiently due to the breaking wave-caused complicated turbulence as well as the lack of precise measuring instruments. However, the time history of the water particle velocity shows an unsymmetrical profile like the water surface profile, as indicated in Fig. 7. Figure 7 shows that the steeper beach slope produces a larger on-offshore velocity than the gentle slope, for a given wave. Kemp[28], however, pointed out from his indoor experiments that the ratio of the maximum onshore velocity to the maximum offshore velocity and the ratio of the duration time of onshore velocity to the duration time of offshore velocity increase with decreasing the beach slope.

4. 2. Irregular wave

The breaking water depth, breaking wave height, and wave steepness have been discussed by Collins[29], Battjes[30, 31], Kuo and Kuo[32], Nath and Ramsey[33], Goda[34], Sawaragi and Iwata, Iwagaki and Kimura[35], and Weishar and Byrne. In dealing with the irregular wave, the zero-upcrossing method or zero-downcrossing method has been used to define the irregular wave from the statistic point of view.

Generally, experimental data defined by the zero-upcrossing method are more scattering than those defined by the zero-downcrossing method. One example is shown in Fig. 8. Fig. 8 shows that the standard deviation of H_b/h_b defined by the zero-downcrossing method is 0. 094 for the spilling breaker and 0. 111 for the plunging

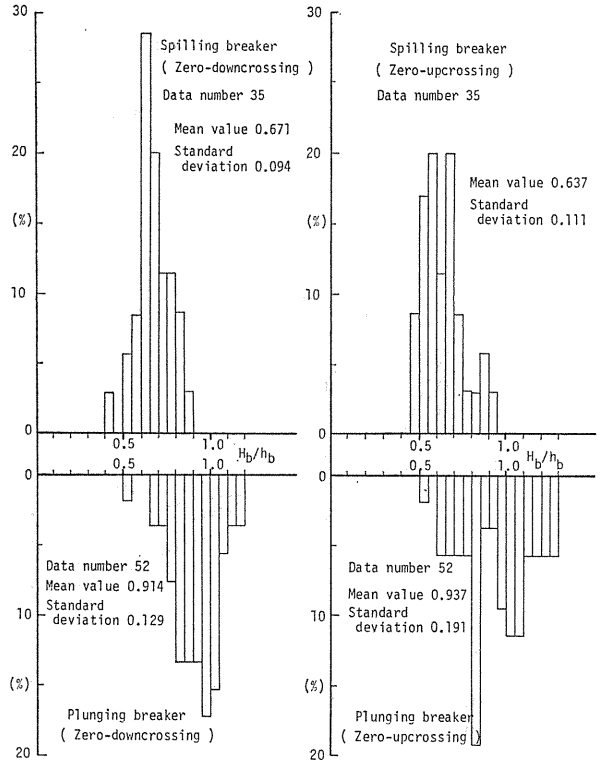

Fig. 8. Frequency of relative breaking wave height.

breaker. On the other hand, the standard deviation of H_b/h_b defined by the zero-upcrossing method is 0. 129 for the spilling breaker and 0. 191 for the plunging breaker. Therefore, it can be said that the zero-downcrossing method is better than the the zero-upcrossing method to describe the wave at the breaking point. Adding to this, it will be shown later that the zero-downcrossing method is better than the zero-upcrossing method to describe small turbulent waves caused by wave breaking. Therefore, the zero-downcrossing method is recommended to define the wave in the surf. Hereafter, the zero-downcrossing method is used to discuss waves in surf.

Let us discuss the wave properties at the breaking point. The relative breaking wave height H_b/h_b seems to be a function of shallowness h_b/L_o, as in Fig. 9, although experimental data are scattering. But, grouping H_b/h_b for the same breaker type, H_b/h_b listed in Table 1 are obtained. The values in Table 1 is

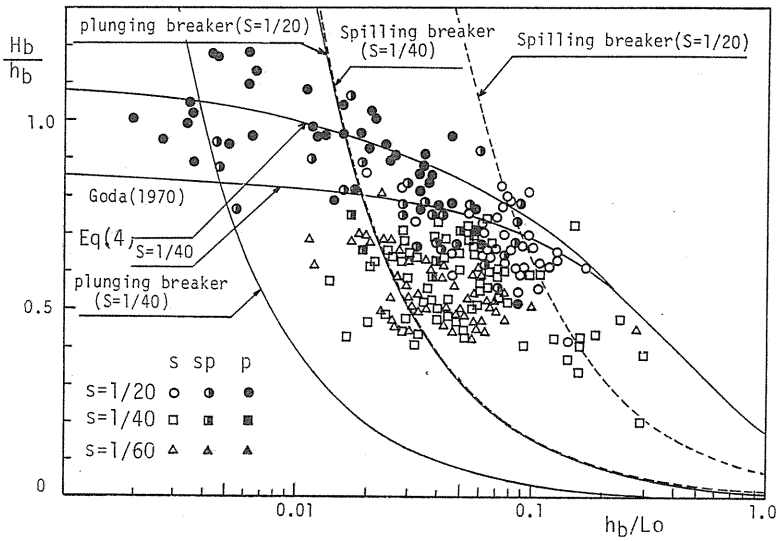

Fig. 9. Relative breaking wave height (irregular wave).

Table 1. Value of relative breaking wave height H_b/h_b for spilling and plunging breakers.

Beach slope	Breaker types	H_b/h_b	Standard deviation	Number of waves
1/20	Spilling breaker Plunging breaker	0.671 0.914	0.094 0.129	35 52
1/40	Spilling breaker	0.584	0.112	83
1/60	Spilling breaker	0.538	0.080	57

different from $H_b/h_b=0.63$ proposed by Kuo and Kuo. In Fig. 9, Eq. (4) is drawn for comparison. The experimental trend that H_b/h_b becomes larger with increase of the beach slope and decrease of h_b/L_o corresponds roughly to Eq. (4). However, experimental values are generally much smaller than Eq. (4). The same thing can be pointed out for a relation of Y_b/h_b and h_b/L_o as indicated in Fig. 10, where Y_b is the wave crest height from the sea bottom. Therefore, it is clear that an individual wave composing the irregular wave can break more easily than the regular wave which has the same wave height and period as the individual wave.

The wave steepness H_b/L_b of the individual wave at the breaking point can be predicted by the critical wave steepness for the regular wave as indicated in Fig.

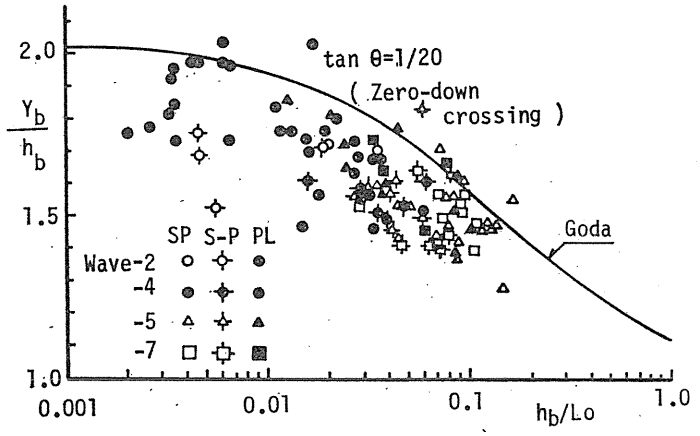

Fig. 10. Relative breaking wave crest height (irregular wave).

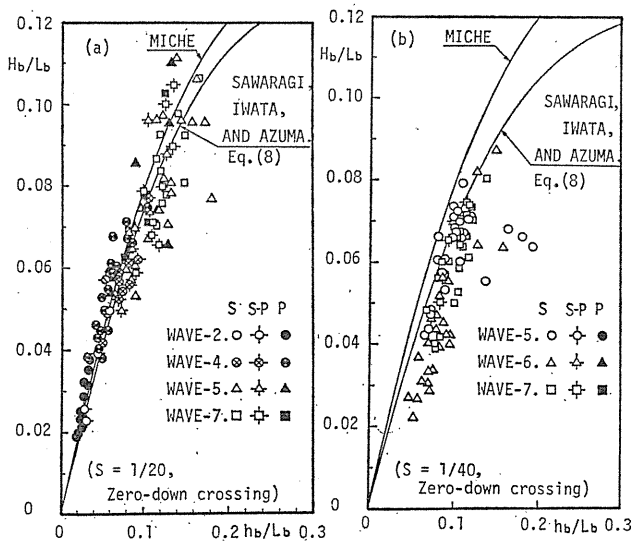

Fig. 11. Breaking wave steepness (irregular wave).

11. In the figure, Eq. (8) is proposed by the present authors.

$$H_b/L_b=(0.362\tan\theta+0.115)\tanh(2(h_b+\eta)/L_b). \tag{8}$$

Generally, Eq. (8) can predict the wave steepness better than Eq. (2) with decreasing of the slope.

Weishar and Byrne showed that Eq. (9) presented by Komar and Gaughan[36]

can estimate well the breaking wave height,

$$H_b=0.39g^{1/5}(H_o^2T_b)^{2/5}. \tag{9}$$

Fig. 12 indicates a relation between H_b and $g^{1/5}(H_0^2T_b)^{2/5}$ for the authors experimental values, where H_o is calculated by the linear wave theory. The correspondence between Eq. (9) and experiments is very good. The problem in using Eq. (9) is the way to estimate H_o from a measured value of H_b. As far as the wave

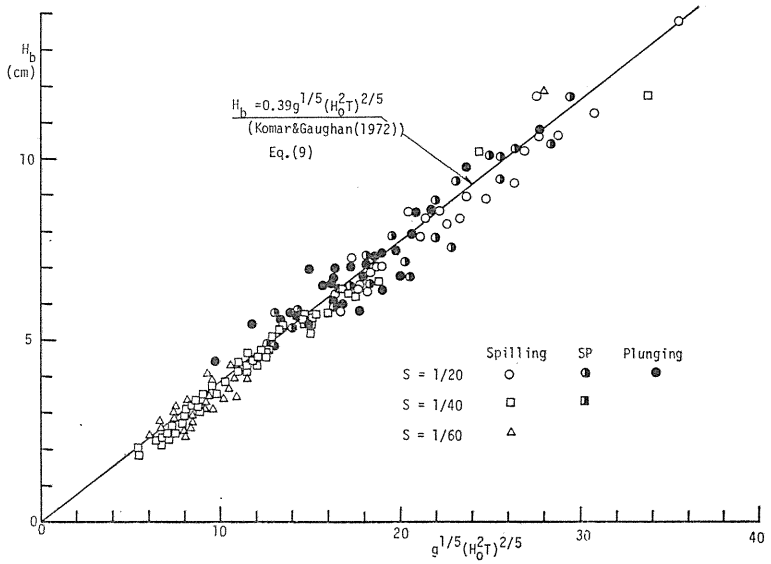

Fig. 12. Relation between H_b and $g^{1/5}$ $(H_o{}^2T)^{2/5}$.

energy conservation based on the linear wave theory is used in order to calculate H_o, the well agreement between experiments and Eq. (9) is expected. Then, the propriety of the above-cited calculation must be made clear in the future study. In the same way, if H_o and T_b are assumed to be calculated from H_b and L_b or T_b by the energy conservation using the linear wave theory, the relative breaking wave height H_b/H_o can be predicted by Eq. (10) as indicated in Fig. 13.

$$H_b/H_o=0.65\tan\theta^{1/2}(H_o/L_o)^{-1/4}+0.32,$$
$$\text{for } 0.9\leq\tan\theta(H_o/L_o)^{-1}/^4\leq3.8. \tag{10}$$

As indicated in Fig. 13, Eq. (10) estimates lower values than those of Eq. (11) proposed by Méhauté-Koh for the regular wave. This fact also shows that the individual wave composing the irregular wave breaks more easily than the regular wave which has the same wave height and period as the individual wave.

$$H_b/H_o=0.76\tan\theta^{1/4}(H_o/L_o)^{-1/4}. \tag{11}$$

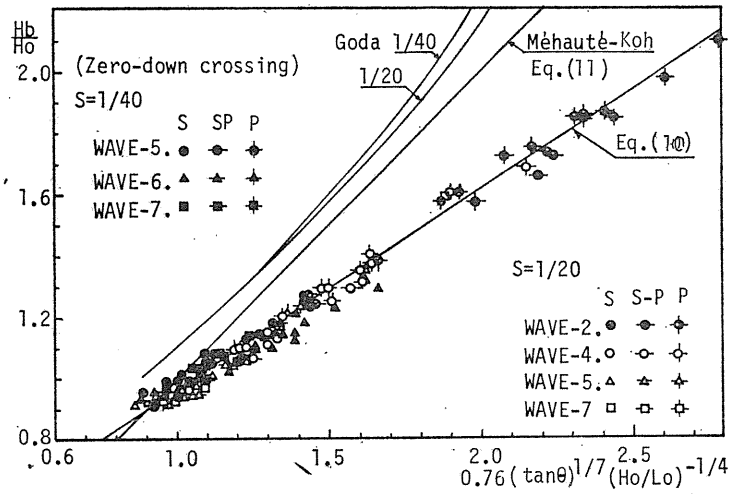

Fig. 13. Relative breaking wave height H_b/H_o (irregular wave).

5. Internal mechanics of breaking wave

In dealing with the wave transformation after breaking, the internal mechanics of breaking wave, in particular the turbulence which is caused by breaking wave has to be made clear. So far, many theoretical models on the breaking wave-caused turbulence have been proposed by many investigators. The laboratory observation made by the present authors[37] revealed that the wave transformation is very different between the spilling breaker and the plunging breaker. That is, the plunging breaker drops its crest to the stillwater level and follows an air-entrained horizontal roller and a splash as shown schematically in Fig. 14. Air is entarined deeply into the water by the horizontal roller and most of the air goes up to the water surface as the roller disappears, and then the air disappears soon.

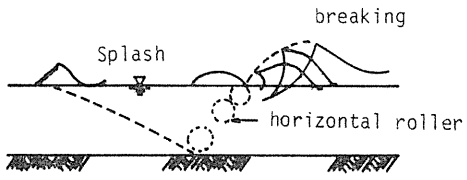

Fig. 14. Schematic illustration of plunging breaker.

On the other hand, the spilling breaker never follows the horizontal roller, and air-bubbles and turbulent water spill down front face of wave (see Fig. 14). The difference of breaker patterns between the spilling breaker and the plunging breaker results in the fact that the wave height decay of the plunging breaker is much larger than that of the spilling breaker. This situation is illustrated in Fig. 15. The present authors calculated the energy dissipation due to the horizontal roller by using a Rankine-type vortex model confirmed by their experiments, and they found that 30% of the energy dissipation due to the wave breaking was brought by the horizontal roller and the rest portion of 70% was attributed to another mechanics, which will be described in the next section.

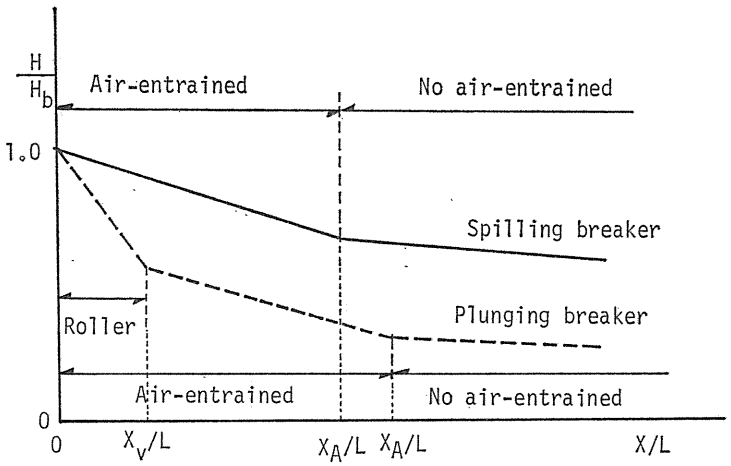

Fig. 15. Schematic illustration of wave height attenuation.

Führböter[38] presented a numerical model in order to calculate the effect of the entrained air-bubble to the energy dissipation caused by the wave breaking. The wave height attenuation calculated by his model is, however, much larger than the experimental facts. Therefore, the model was not so helpful to estimate the wave energy dissipation by wave breaking.

Peregrine[39] tried to study the turbulence of the wave breaking by a flow-visualization method. He pointed out that the surface turbulence on the front surface of wave is not an important factor, and he insisted that the flow pattern due to wave breaking was very similar to the turbulent mixing layer.

Various investigations on the breaking wave-caused turbulence have been performed, as described above. We have to formulate the turbulence in order to estimate the wave height attenuation from theories which will be discussed in the next section. However, since the turbulence caused by the wave breaking is very different among breakers, its formation is very difficult. The concept of the wall turbulence or bore model has been adopted in calculating the wave height from theories.

The concept of the wall turbulence was used by Horikawa and Kuo[40], and the present authors[41] in their theoretical development to estimate the wave height attenuation after breaking. Horikawa and Kuo assumed the turbulence to be isotropic. They developed a theory by using the isotropic turbulence model as well as by using the assumption that the wave energy dissipation decreases exponentially with wave propagation. On the other hand, The present authors assumed that Reynolds stresses of the turbulence caused by the wave breaking, P_{xx} and P_{xz} can be expressed by Prandtle-type expression as follows;

$$\left.\begin{aligned} P_{xx} &= -\rho l_x \frac{\partial u}{\partial x}\left|\frac{\partial u}{\partial x}\right| \\ P_{xz} &= -\rho l_z \frac{\partial u}{\partial z}\left|\frac{\partial u}{\partial z}\right| \end{aligned}\right\}. \tag{12}$$

In Eq. (12), P_{xx} is the normal stress acting on a vertical plane perpendicular to the wave propagation direction (x-axis), P_{xz} is the shear stress acting on a horizontal plane perpendicular to z-axis, ρ is the density of water, l_x and l_z are mixing lengths, and u is the horizontal velocity of water particle.

The present authors assumed the following relation for the turbulence with air entrainment in the surf,

$$\frac{\partial u}{\partial x} \propto u/L \quad \text{and} \quad \frac{\partial u}{\partial z} \propto u/h. \tag{13}$$

From Eq. (13), P_{xx} and P_{xz} are given by

$$\left.\begin{aligned} P_{xx} &= -\rho L_x^2 (u/L)^2, \\ P_{xz} &= -\rho L_z^2 (u/h)^2. \end{aligned}\right\} \tag{14}$$

In Eq. (14), L is the wave length at the depth of h, h is the stillwater depth. L_x and L_z indicating x and z components of the turbulence respectively are connected to the turbulence scale L_B by

$$L_B = \sqrt{\alpha L_x^2 + \beta L_z^2}, \tag{15}$$

where, α and β are constants satisfing the following relations,

$$\begin{aligned} &L = (h/\alpha), \\ &\frac{\partial}{\partial z}[\rho L_z^2 (u/h)^2] = \beta \frac{\partial}{\partial x}[\rho L_z^2 (u/h)^2]. \end{aligned} \tag{16}$$

Furthermore, they assumed L_B in Eq. (15) as follow,

$$L_B = m(h+\eta), \tag{17}$$

where, m is a constant. Battjes[31] used the concept of bore. He adopted the bore model proposed by Le Méhauté[42], as in Fig. 16. Based on the conservation of mass and momentum fluxes, the energy dissipation D' per one wave length due to the bore model is given by

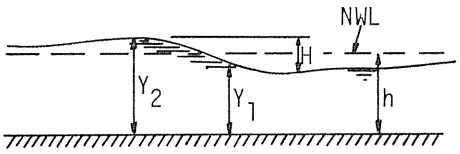

Fig. 16. Bore model.

$$D' = \frac{1}{4}\rho g (Y_2 - Y_1)^3 \left[\frac{g(Y_1+Y_2)}{2Y_1Y_2}\right]^{1/2}, \tag{18}$$

where, Y_1 and Y_2 are water depths (see Fig. 16).

Following relationships,

$$\begin{aligned} &Y_2 - Y_1 \cong H, \\ &\left[\frac{g(Y_2-Y_1)}{2Y_1Y_2}\right]^{1/2} \propto \left(\frac{g}{h}\right)^{1/2}, \end{aligned} \tag{19}$$

D' is transformed to

$$D'=\frac{1}{4}\rho g H^3\left(\frac{g}{h}\right)^{1/2}. \tag{20}$$

When the wave is periodic and its frequency is f $(=1/T)$, the average energy dissipation D per unit area is given by

$$D=D'/L=fD'/C\propto fD'/(gh)^{1/2}\propto \frac{1}{4}f\rho g\frac{H^3}{h}, \tag{21}$$

where, C is the wave celerity. The equation (21) is the turbulence model presented by Battjes.

6. Wave deformation after breaking

As described in the previous section, wave deformation after breaking is closely related to the horizontal roller, bottom friction and the so-called turbulence produced by wave breaking.

6. 1. Wave energy dissipation due to horizontal roller

The distribution of angular velocity of the roller is approximated as a Rankine type vortex as indicated in Fig. 17[41]. The angular velocity takes a maximum value at $r=r_o$, and experimental values in Fig. 18 show

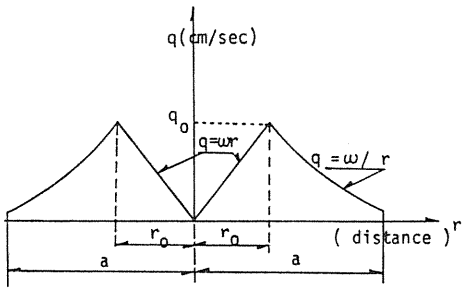

Fig. 17. Rankine type vortex.

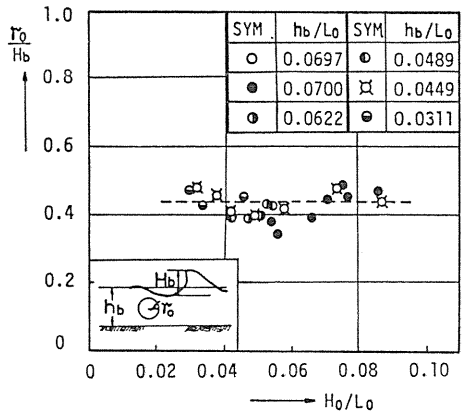

Fig. 18. Radius of horizontal roller.

$$r_o=0.44\,H_b. \tag{22}$$

Now, next consider the effect of the horizontal roller on wave energy dissipation. The kinematic energy, E_r of the horizontal roller is defined by

$$E_r=\frac{1}{4}\rho\pi(q_o r_o)^2(1+4\ln(a/r_o)), \tag{23}$$

where, q_o is the angular velocity at $r=r_o$, and ρ is the density of water. If the energy of breaking wave can be expressed as that before breaking, the energy dissipation E_L from the breaking point to the point where the roller disappears is given by

$$E_L=\frac{1}{8}\rho g(H_b^2-H_v^2)L, \tag{24}$$

where, H_v is the wave height at the point where the roller disappears. Therefore, the ratio of E_r to E_L is given by

$$\varepsilon_r=\frac{E_r}{E_L}=\frac{1.216q_0^2(1+4\ln(a/r_o))}{gL(1-(H_v/H_b)^2)}. \tag{25}$$

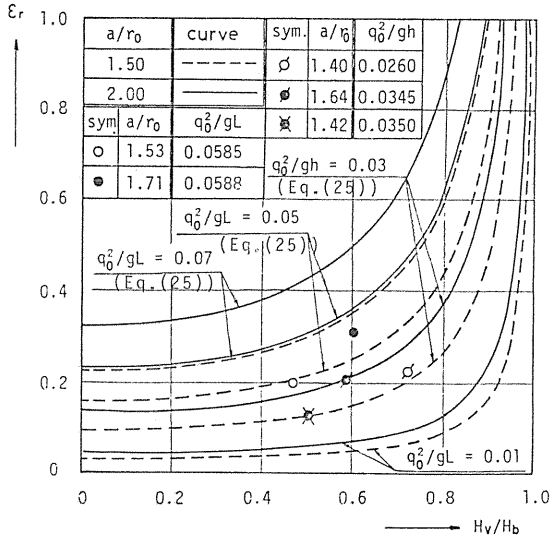

Fig. 19. Energy loss due to horizontal roller.

In deducing Eq. (25), Eq. (22) is used. Fig. 19 presents the theoretical values of Eq. (25) and experimental results. The theoretical values show that ε_r increases with increase of q_o^2/gL and a/r_o. The experimental values indicate that 15%~30% of the total wave energy dissipation is transmitted to the kinematic energy of the roller. Therefore, it is concluded that most of the wave energy is dissipated by other factors such as bottom friction, splash, and air-entrained turbulence, etc..

6. 2. Effect of bottom friction on wave energy dissipation

A bottom shear stress due to wave motion was measured by the shear meter devised by the authors.[41] A schematic view of the shear meter is given in Fig. 20. A small raised channel was set transversely from wall to wall of the frame below the shear plate. To prevent a flow through gaps under the plate, the channel was filled with mercury until its meniscus touches the underside of the shear plate as Eagleson[43] already devised. If the flow under the plate is not stopped,

the pressure gradient is different between above and below the shear plate, which causes the force acting in the opposite direction to the original wave force.

A shear force acting on the shear plate was measured by converting the force into a moment of a supporting shaft. The shear plate is subjected to a force due to wave pressure gradient in addition to the shear force. Therefore, the force due to the pressure gradient is calculated from the pressure difference measured by pressure measuring tubes. Before measuring the bottom friction force due to breaking waves, the shear meter was checked for various conditions where the flow is laminar, and it was recognized that measurements coincides well with theoretical values calculated by the theory of Iwagaki et al..[44]

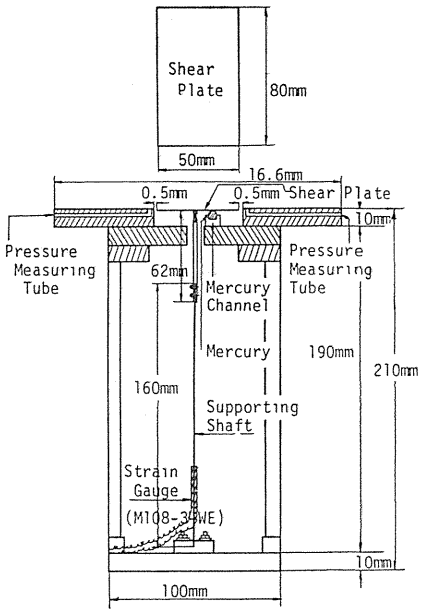

Fig. 20. Schematic view of shear meter.

6. 2. 1. Bottom friction coefficient

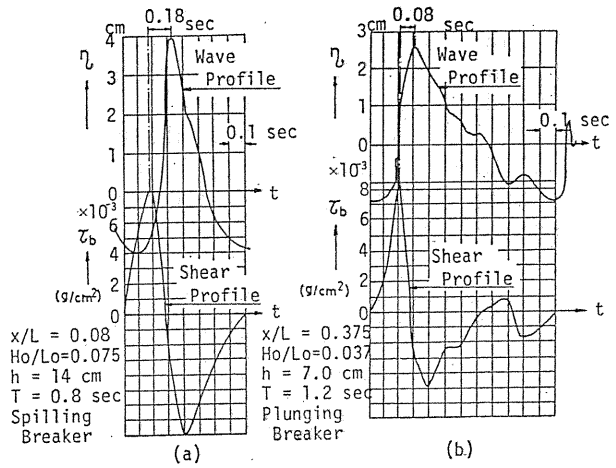

Fig. 21. Time history of shear stress and water surface profile.

Fig. 21 shows two examples of time profiles of a bottom shear stress and a wave. The figure presents that the time profiles of shear stress of the plunging breaker is very asymmetrical as compared with those of the spilling breaker. Fig. 22 shows a change of non-dimensional maximum bottom shear stresses acting in the wave propagation direction and its reverse direction for two types of break-

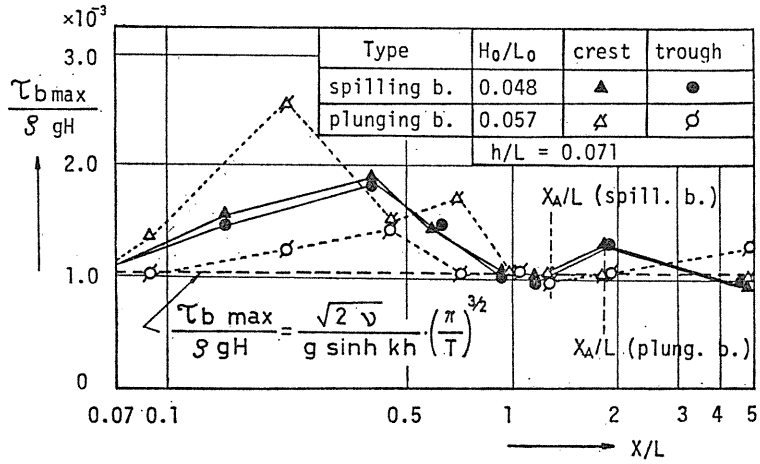

Fig. 22. Examples of relation between $\tau_{b\ \max}/\rho gH$ and X/L.

ers. In Fig. 22, x is the distance from the breaking point and the dotted lines express the shear stress estimated by the smooth laminar boundary layer theory[44] given by

$$\frac{\tau_b \max}{\rho g H} = \frac{\sqrt{2\nu}}{g \sin h(kh)} \left(\frac{\pi}{T}\right)^{3/2}. \tag{26}$$

where, ν is the kinematic fluid viscosity, $\tau_{b\max}$ is the maximum bottom shear stress, $k=2\pi/L$, ρ is the fluid density, and H is the wave height at the depth of h. The maximum bottom shear stress in the region for $x \leqq x_A$ is usually considerably larger than that in the range for $x > x_A$, where x_A is the distance where the air-bubble disappears from the water body from the breaking point. Therefore, it is clear that the bottom shear stresses become larger due to air-entrained turbulence. As indicated in Fig. 21, the time profile of the bottom shear stresses are very asymmetrical and then the coefficient of the bottom friction which was defined earlier cannot be applied directly. Then, a coefficient of the bottom friction $\hat{C}_f$ is defined newly here as follow,

$$\hat{C}_f = \frac{1}{2\pi}(\theta_c \hat{C}_{fc} + \theta_t \hat{C}_{ft}), \tag{27}$$

$$\hat{C}_{fc} = 2|\tau_{bc}|/|U_{bc}^2|,$$

$$\hat{C}_{ft} = 2|\tau_{bc}|/|U_{bt}^2|, \tag{28}$$

$$\theta_c + \theta_t = 2\pi,$$

where, θ is the phase, U_b is the horizontal particle velocity at bottom, τ_b is the bottom shear stress, subsuffix c and t express the direction of wave propagation and antiwave propagation, respectively, and the super bar indicates a time averaging value.

The coefficient of the bottom friction C_f does not show a clear correlation with the distance of wave propagation from the breaking point, as in Fig. 23. Fig.

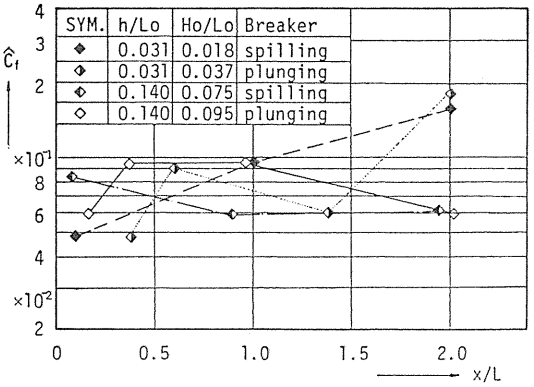

Fig. 23. Changes of coefficient $\hat{C}_f$ with X/L.

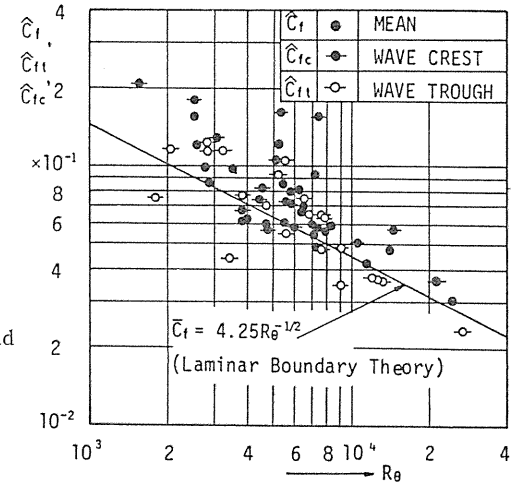

Fig. 24. Relations among $\hat{C}_f$, $\hat{C}_{ft}$, $\hat{C}_{fc}$ and R_θ.

24 indicates a relation among $\hat{C}_f$, $\hat{C}_{ft}$, $\hat{C}_{fc}$ and Reynolds number R_e. The Reynold number is defined here by

$$R_e = U_b^2 T/\nu \tag{29}$$

where, T is the wave period and U_b is the mean value of horizontal water particle velocity at bottom. $\hat{C}_f$, $\hat{C}_{ft}$ and $\hat{C}_{fc}$ are generally recognized to increase with decreasing of R_e. Experimental value of C_f are, however, generally higher than the theoretical value given by Eq. (30) which is based on the smooth laminar boundary theory.[44]

$$C_f = 4.5 R_e^{-1/2}. \tag{30}$$

Therefore, the bottom friction cannot be predicted by the smooth laminar boundary theory. By the way, the bottom friction coefficient f which has been used especially in the field observations is defined as follow[41],

$$f = \tau_{b\max}/\rho {U_b}^2{}_{\max}, \tag{31}$$

where, $\tau_{b\,max}$ is the maximum bottom shear stress, $U_{b\,max}$ is the maximum horizontal particle velocity at bottom. Fig. 25 shows a relation between f and Reynolds number R_{eT} which is defined by

$$R_{eT}=U_{b\,max}^{2}T/\nu. \tag{32}$$

The straight line in the figure 25 is the theoretical value of the smooth laminar boundary layer theory given by

$$f=2.08R_{eT}^{-1/2}. \tag{33}$$

Experimental values after wave breaking in Fig. 26 are generally 2~4 times larger than the theoretical value. Therefore, it can be concluded that the smooth laminar boundary theory cannot be applied to breaking waves. A new theory must be developed.

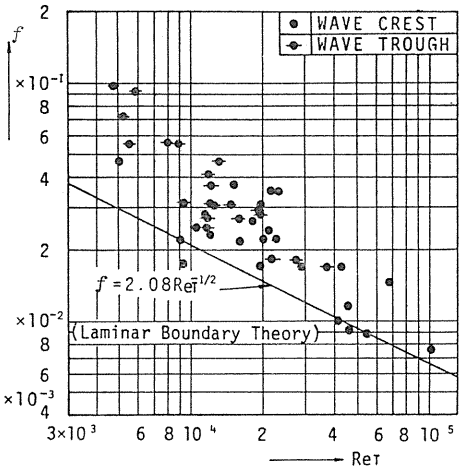

Fig. 25. Relation between f and R_{eT}.

6. 2. 2. Energy dissipation due to bottom friction

Let us discuss the energy dissipation due to bottom friction. The mean energy dissipation, $\overline{E}_{fb}$ due to the bottom friction per unit area is given by

$$\overline{E}_{fb}=\frac{1}{T}\int_{0}^{T}\overline{U}_{b}\overline{\tau}_{b}dt, \tag{34}$$

where, $\overline{U}_{b}$ and $\overline{\tau}_{b}$ are respectively the mean value of horizontal particle velocity and the shear stress at the bottom, and the mean value is taken for the same sign.

From the energy conservation law, the following relation is derived,

$$\frac{d}{dx}(C_{g}E)=\overline{E}_{fb}+\overline{E}_{ft}. \tag{35}$$

In Eq. (35), C_{g} is the group velocity, E is the wave energy per unit area, and $\overline{E}_{ft}$ is the mean energy loss due to turbulence excluding the bottom friction. We have no perfect expression for C_{g} and E after wave breaking, therefore C_{g} and E are assumed to be given by the small amplitude wave theory;

$$\left.\begin{aligned} C_{g}&=C\\ E&=\frac{1}{8}\rho gH^{2}\end{aligned}\right\}, \tag{36}$$

where, C is the wave celerity.

The ratio of the energy loss due to the bottom friction to the total energy loss for the distance of dx is expressed by,

$$\varepsilon=\frac{\overline{E}_{fb}}{\frac{d}{dx}(C_gE)}=\frac{4\int_0^T\overline{\tau}\overline{U}_b dt}{gHTC(dH/dx)} \tag{37}$$

Table 2. Energy loss due to bottom friction

RUN	h cm	T sec	H_b cm	H cm	X/L	$C/\sqrt{gh}$	$\varepsilon\times10^2$	Breaker
5	7	1.2	5.0	4.4	0.25	1.07	0.8	spilling
〃	〃	〃	〃	2.7	1.40	0.97	4.0	〃
〃	〃	〃	〃	2.6	2.10	0.94	8.9	〃
6	7	1.2	8.0	5.0	0.30	1.07	0.6	plunging
〃	〃	〃	〃	3.2	1.50	1.14	4.2	〃
〃	〃	〃	〃	2.7	2.20	1.03	5.5	〃
13	14	0.8	6.3	5.4	0.85	0.87	1.7	spilling
〃	〃	〃	〃	4.9	1.30	0.99	2.2	〃
〃	〃	〃	〃	4.6	2.00	0.94	7.7	〃
14	14	0.8	9.5	5.4	0.95	0.94	1.0	plunging
〃	〃	〃	〃	5.0	1.30	0.99	1.9	〃
〃	〃	〃	〃	4.7	2.05	0.94	2.6	〃

The ratio ε is calculated easily by using experimental values for the wave height attenuation and the shear stress. Table 2 indicates the calculated values of ε. From the table, it is clear that the energy loss due to the bottom friction is quite small, i. e. within the distance of twice the wave length from the breaking point in which the wave height attenuation is remarkably large, the ratio of the wave energy dissipation due to bottom friction to the total wave energy loss is about 9 % at most. As far as the assumption of Eq. (36) is established, the contribution of the bottom friction to the wave energy decay after wave breaking is quite small and it may safely be said that the bottom friction is not taken into consideration for discussing the wave decay after wave breaking.

Combining the discussion of previous section and the present section, it can be concluded that the energy dissipation due to the horizontal roller and the bottom friction is much smaller than the actual wave energy loss. Therefore, it will be suggested that the so-called turbulence with air-entrainment is an important factor for the wave energy attenuation after wave breaking.

6. 3. Turbulence of water surface profile

The breaker-caused turbulence is so strong that the water surface profile in the surf is very rough, different from a smooth symmetrical surface profile before wave breaking. The characteristics of the turbulence including the water particle

velocity field have not made clear. In this section, turbulence of the water surface profile is discussed.

6. 3. 1. Regular wave

The present authors[45] revealed by experiments that a monochromatic wave is transformed to be a complicated wave composed of many high frequency component waves due to the non-linearity of wave breaking, as indicated in Fig. 26. In Fig. 26, x is the distance with the origin of the breaking point and its positive direction is shoreward, and f_0 is the predominant frequency of an incident wave. Based on a dimensional analysis, the present authors discussed the variation of wave height spectrum $H(f)$, where f is the wave frequency.

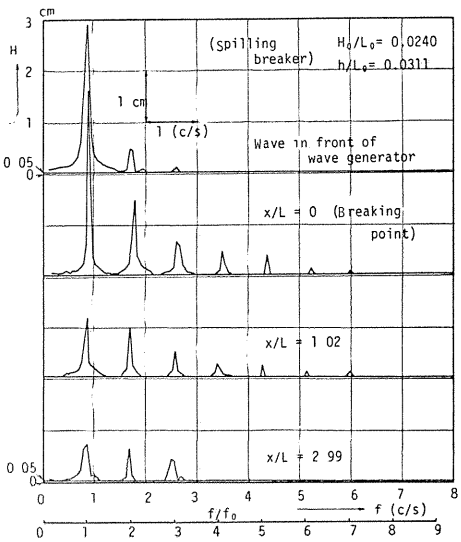

Fig. 26. Variation of wave height spectrum.

The physical qunatities to be considered in the dimensional analysis of the wave height spectrum $H(f)$ are the gravitational acceleration g, the wave frequency f, the stillwater depth h, the density of water with air-entrainment ρ^*, the molecular viscosity of water with air-entrainment μ^*, and the surface tension κ as given in Eq. (38),

$$H(f)=F[g,\ f,\ h,\ \rho^*,\ \mu^*,\ \kappa]. \tag{38}$$

The significance of these 6 physical quantities changes according to the frequency ranges of the very shallow water wave, the shallow water wave, the deep water wave, the capillary wave and the frequecy range in which the viscosity is predominant. Then, selecting important parameters to represent the each frequency range and determining the combination of the chosen parameters to have the dimension $[L]$ of the wave height spectrum $H(f)$, the following relations are derived;

(1) frequency range of the very shallow water wave;

$$f\leq f_1 \text{ (see Fig. } -27),$$
$$H(f)=F_1[h,\ f]=B_1h, \tag{39}$$

(2) frequency range of the shallow water wave;

$$f_1<f\leq f_2,$$
$$H(f)=F_2[h,\ g,\ f]=B_2(gh)^{1/2}f^{-1}, \tag{40}$$

(3) frequency range of the deep water wave;

$$f_2 < f \leq f_3,$$

$$H(f) = F_3[g,\ f] = B_3 g f^{-2}, \tag{41}$$

(4) frequency range of the capillary wave;

$$f_3 < f \leq f_4,$$

$$H(f) = F_4[f,\ \rho^*,\ \kappa] = B_4 \kappa^{1/3} \rho^{*-1/3} f^{-2/3} \tag{42}$$

(5) frequency corresponding to the viscosity;

$$f_4 < f,$$

$$H(f) = F_5[\rho^*,\ \mu^*,\ f] = B_5 \rho^{*-1/2} \mu^{*1/2} f^{-1/2}. \tag{43}$$

In Eqs. (39)$\sim$(43), f_1 is given by

$$f_1 = (g/625h)^{1/2}, \tag{44}$$

which is deduced by the following equation,

$$h/L = 0.04. \tag{45}$$

The frequency f_2 is given by Eq. (46) which satisfies Eq. (47),

$$f_2 = (g/4\pi h)^{1/2}, \tag{46}$$

$$h/L = 0.5. \tag{47}$$

f_3 is the critical frequency between the gravity wave and the capillary wave;

$$f_3 = \frac{1}{2\pi}(\rho g^3/\kappa)^{1/4}. \tag{48}$$

The frequency f_4 is unknown. $B_1 \sim B_5$ including in Eqs. (39)$\sim$(43) are dimensionless coefficients.

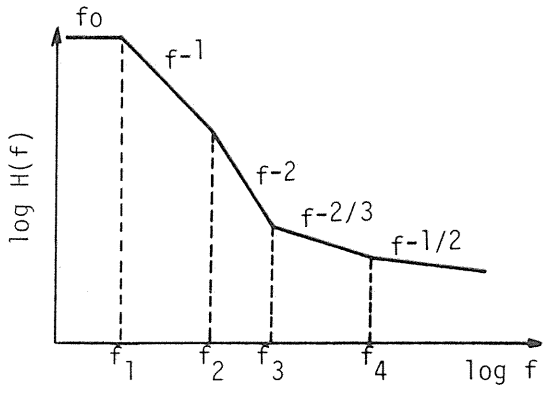

Fig. 27. Schematic illustration of equilibrium spectral slope.

Fig. 27 shows the model of the wave height spectrum given by Eqs. (39)～(43). Fig.28 indicates that the proposed spectrum slopes corresponds well to the exepriments in the frequency range where the gravitational acceleration is predominant, $f_3 \geq f \geq f_1$.

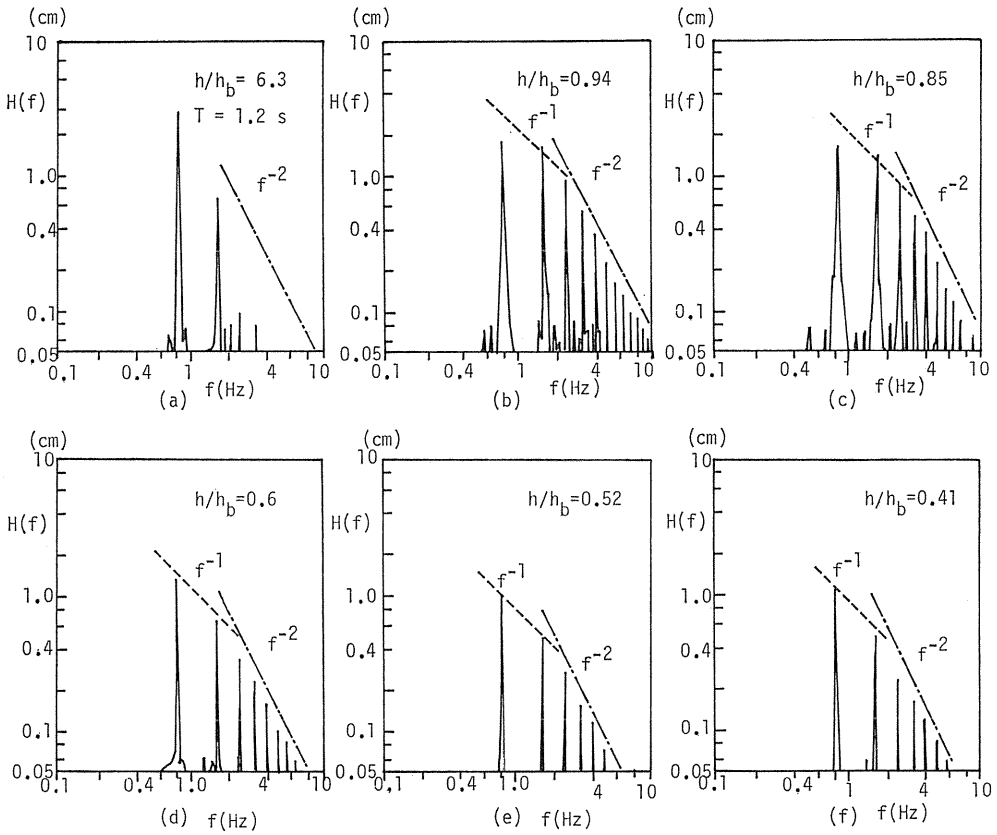

Fig. 28. Variation of wave height spectrum on sloping bed.

6. 3. 2. Irregular wave

The variation of wave power spectrum $S(f)$ (frequency spectrum) is discussed in this section. The dimension of $S(f)$ is $[L^2T]$.

6. 3. 2. 1. Case considering no return flow

Based on a dimensional analysis, the present authors[46] discussed the slopes of the wave power spectrum in the surf. The procedure adopted are the same as the case of the regular wave. The spectral slopes proposed are as follows;

(1) $f \leq f_1$ ($h/L \leq 0.04$; the very shallow water wave),

$$S(f) = K^1 h^2 f^{-1}, \qquad (49)$$

where, $f_1 = (g/625h)^{1/2}$

(2) $f_1<f<f_2$ $(0.04<h/L<0.5$; the shallow water wave),

$$S(f)=K_2ghf^{-3},$$
$$\text{where,}\quad f_2=(g/4\pi h)^{1/2}. \tag{50}$$

(3) $f_2\leq f<f_3$ $(h/L\geq 0.5$; the deep water wave),

$$S(f)=K_3g^{-2}f^{-5},$$
$$\text{where,}\quad f_3=\frac{1}{2\pi}(g^3\rho/\kappa)^{1/4}. \tag{51}$$

In Eqs. (49)$\sim$(51), $K_1\sim K_3$ are unknown dimensionless coefficients.

6. 3. 2. 2. Case considering the return flow

When the velocity of the return flow U is considered, the following relations can be deduced in place of Eqs. (49)$\sim$(51),

$$\text{(1)}\quad S(f)=K_4Uhf^{-2};\ f\leq f_1, \tag{52}$$

$$\text{(2)}\quad S(f)=K_5U(gh)^{1/2}f^{-3};\ f_1<f\leq f_2, \tag{53}$$

$$\text{(3)}\quad S(f)=K_6Ugf^{-4};\ f_2<f\leq f_3. \tag{54}$$

In Eqs. (52)$\sim$(54), $K_4\sim K_6$ are unknown dimensionless coefficients. The effect of the return flow to the wave is predominant near the shoreline, according to experiments on regular waves. Therefore, it will be understood that Eqs. (52)$\sim$(54) appears on waves near the shoreline.

6. 3. 2. 3. Equilibrium spectral slope

Summarizing the above-mentioned in the previous two sections of *6. 3. 2. 1* and *6. 3. 2. 2*, the following transformation process of the wave power spectrum shape can be said. As a random wave, of which equilibrium spectral slope is proportional to "f^{-5}" predicted by Phillips[47] (see Fig. 29 (a)), propagates into shallow water depth, it experiences a depth-limitted wave breaking and forms the so-called surf zone. The spectral slope corresponding to the shallow water waves

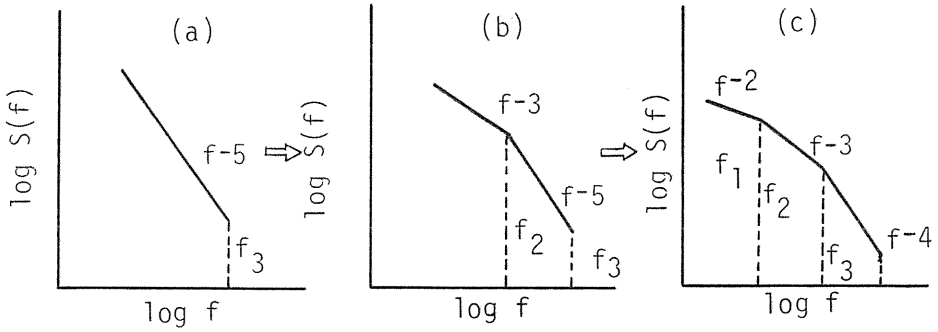

Fig. 29. Variation of equilibrium spectral slope.

will show the equilibrium slope of "f^{-3}" and then the spectral slope on high frequency range will be composed of "f^{-3}" and "f^{-5}", as indicated in Fig. 29(b). However, in this stage, the spectral slope of "f^{-1}" given by Eq. (49) is not supposed to appear. As the random wave advances further into shallow water depth, the wave-induced return flow will play an important role in shaping the power spectral slope and finally the spectral slope on the high frequency band will be constructed by "f^{-2}", "f^{-3}" and "f^{-4}", as indicated in Fig. 29 (c).

Fig. 30 shows one experimental result on the change of the wave power spectrum in an irregular wave on the beach slope of 1/40 performed by the present

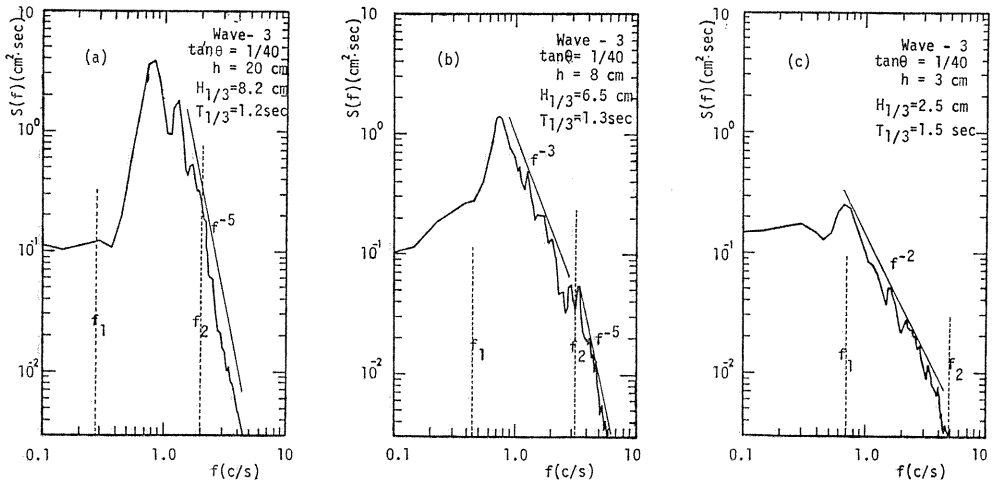

Fig. 30. Variation of wave power spectrum.

authors[46]. In Fig. 30 (a), the spectral slope on high frequency is proportional to "f^{-5}", because the wave is outside the shallow water surf. Fig. 30 (b) shows the wave at the depth of 8 cm in the shallow water surf has the spectral slope proportional to "f^{-3}" and "f^{-5}" as an equilibrium slope. The spectral slope, however, becomes flatter than "f^{-3}" at the depth of 3 cm and is almost proportional to "f^{-2}". This will imply that the proposed spectral slope based on the dimensional analysis is not an universal shape inside the the surf-zone.

Besides the present authors' study[46], there are other investigations on the change of wave power spectrum shape. Ijima[48] proposed an equilibrium spectral slope of "f^{-1}" and "f^{-5}" for the frequency corresponding to the long and deep water waves, respectively. Kitaigordskii[49] presented an equilibrium spectral slope proportional to "f^{-3}" and "f^{-5}" for the corresponding frequencies mentioned above. On the other hand, Thornton[50] pointed out in his field measurement that the spectral slope for high frequencies is proportional to "f^{-3}".

6. 4. *Analytical method*

What we have a strong interest in wave characteristics after wave breaking is the variation of wave height. Since the mechanics of wave breaking and wave breaking-induced turbulence have not yet been clarified, some modellings on the turbulencence have been set up in order to develop wave theories. Generally, there

are two methods in the theoretical treatments; (a) analytical method and (b) energy method.

The analytical method is an orthodox method which solves the basic equation by numerical calculation by means of the characteristics method, or the finite-different scheme, etc., because the basic equation is non-linear. On the other hand, the energy method calculates the wave deformation by use of the energy balance equation. The energy method usually takes advantage of a specific wave having an unchangeable wave form such as a solitary wave and bore; therefore, the variation of water surface profile cannot be discussed by the energy method.

Let us first deal with an analytical method. The analytical method described hereafter is proposed by the present authors[42].

6. 4. 1. Basic equations

First calculation of the wave deformation on a sloping bottom was carried out by Stoker[51]. He solved numerically a non-linear shallow water wave theory by means of the characteristics method. Since then, some analytical approaches have been proposed. However, most of the approaches were based on non-linear shallow water wave theories and they did not include the turbulence term caused by wave breaking which is discussed in details in the foregoing section. Accordingly, the foregoing analytical approaches did not explain well the wave height attenuation after wave breaking.

The present authors[41] assumed the breaking wave-caused turbulence to be expressed by Eqs. (12)～(17) and calculated the wave height decay by the following basic equation having the turbulence term;

Equation of motion;

$$\rho\frac{Du}{Dt}=-\frac{\partial P}{\partial x}+\mu\nabla^2 u+\left[\frac{\partial P_{xx}}{\partial x}+\frac{\partial P_{xz}}{\partial z}\right],$$
$$\rho\frac{Dw}{Dt}=-\rho g-\frac{\partial P}{\partial z}+\mu\nabla^2 w+\left[\frac{\partial P_{zx}}{\partial x}+\frac{\partial P_{zz}}{\partial z}\right]. \tag{55}$$

Equation of continuity;

$$\frac{D\rho}{Dt}+\rho\left(\frac{\partial u}{\partial x}+\frac{\partial w}{\partial z}\right)=0, \tag{56}$$

where, P_{xx}, P_{xz}, P_{zx}, and P_{zz} are Reynolds stressess, u and w are the horizontal and vertical velocities of water particle, respectively, P is the wave pressure and is given by $P=\rho g(h+\eta-z)$, and η is the water surface profile. Du/Dt and ∇^2 are defined as follows;

$$\frac{Du}{Dt}=\frac{\partial u}{\partial t}+u\frac{\partial u}{\partial x}+w\frac{\partial u}{\partial z},$$
$$\nabla^2=\frac{\partial^2}{\partial x^2}+\frac{\partial^2}{\partial z^2}.$$

Using the following assumptions,

(1) the fluid is incompressible,

(2) P_{zx} and P_{zz} are neglected compared to P_{xx} and P_{xz}, and
(3) P_{xx} and P_{xz} are expressed by Eqs. (12)～(17),
Eqs. (55) and (56) are transformed to

$$\frac{\partial u}{\partial t}+u\frac{\partial u}{\partial x}=-g\frac{\partial \eta}{\partial x}-\frac{\partial}{\partial x}\left(m^2(h+\eta)^2\left(\frac{u}{h}\right)^2\right), \tag{57}$$

$$\frac{\partial \eta}{\partial t}+\frac{\partial}{\partial x}(u(h+\eta))=0. \tag{58}$$

where, m is the constant coefficient defined by Eq. (17) and is called a turbulence constant by the present authors.

6. 4. 2. Numerical calculation

The non-dimensional variables defined by Eq. (59) are used.

$$\begin{aligned} &X^*=x/h, \quad T^*=(t/h)\sqrt{gh}, \quad U^*=u/\sqrt{gh}, \\ &H^*=(h+\eta)/h, \quad M^*=m^2. \end{aligned} \tag{59}$$

Then, the dimensionless forms of Eqs. (57) and (58) are,

$$\frac{\partial U^*}{\partial T^*}+\frac{1}{2}\frac{\partial U^{*2}}{\partial X^*}+\frac{\partial H^*}{\partial X^*}+\frac{\partial}{\partial X^*}(M^*H^{*2}U^{*2})=0, \tag{60}$$

$$\frac{\partial H^*}{\partial T^*}+\frac{\partial}{\partial X^*}(U^*H^*)=0. \tag{61}$$

Eqs. (60) and (61) are used in performing the numerical calculation. The numerical calculation is carried out by the finite difference method (Keller-Levine-Whitham[52]). The finite difference form of Eqs. (60) and (61) presents the following set of equations which estimates the wave height and period.

$$H^*(P)=\frac{1}{2}[H^*(R_1)+H^*(Q_1)]-\frac{\Delta T^*}{2\Delta X^*}[U^*(R_1)H^*(R_1)-U^*(Q_1)H^*(Q_1)], \tag{62}$$

$$\begin{aligned} U^*(P)=&\frac{1}{2}[U^*(R_1)+U^*(Q_1)] \\ &-\frac{\Delta T^*}{2\Delta X^*}\left[\frac{1}{2}(U^{*2}(R_1)-U^{*2}(Q_1))+(H^*(R_1)-H^*(Q_1))\right] \\ &-m\frac{\Delta T^*}{2\Delta X^*}[H^{*2}(R_1)U^{*2}(R_1)-H^{*2}(Q_1)U^{*2}(Q_1)]. \end{aligned} \tag{63}$$

The numerical procedure is, in outline, to compute a wave height and velocity on a set of net points (X_i^*, X_j^*). The unknown values of $H^*(P)$ and $U^*(P)$ at a point P are calculated by use of the known values of $H^*(R_1)$, $H^*(Q_1)$, $U^*(R_1)$

and $U^*(Q_1)$ at points of R_1 and Q_1, as indicated in Fig. 31.

In the calculation, the spatial net and time net are chosen to be uniform uniform; $X_i^*=i\Delta X^*$ and $T_j^*=j\Delta T^*$, where, ΔT^* and ΔX^* are chosen to satisfy a stability condition of the so-called Courant condition[52] stated as follow,

$$T^* \leqq \min_{P_i}\left(\frac{X_*}{U^*(P_i)+(H^*(P_i))^{1/2}}\right). \tag{64}$$

The calculation was done by using the mesh width of $X^*=0.02$ and $T^*=0.004$, for which convergence and stability of the solution were confirmed.

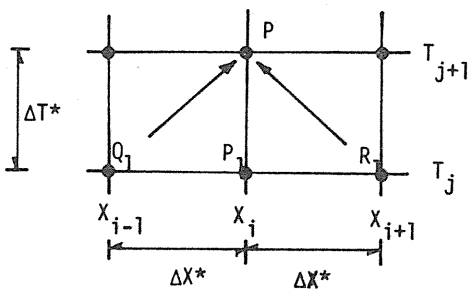

Fig. 31. Mesh point.

In order to calculate the wave height attenuation, the water surface profile and particle velocity at the breaking point are needed as the initial condition. The present authors used both a theoretical wave profile and velocity proposed by Boussinesq and those measured in the present authors' laboratory experiments as the initial condition. Calculated values were shown to have good agreement with experiments for a moderate values of m. Fig. 32 shows a comparison between calculations and experiments, in which the wave profile and water particle velocity measured were used as an initial condition at the breaking point. Suhayda[53] reported that the above-cited calculations of the present authors corresponds well to the field measurements as indicated in Fig. 33. The value of M^* in Fig. 33, however, depends upon the breaker type and cannot be given theoretically at present.

On the other hand, an analytical method for irregualr waves have not yet proposed. Then, the theoretical treatment is left to the future studies.

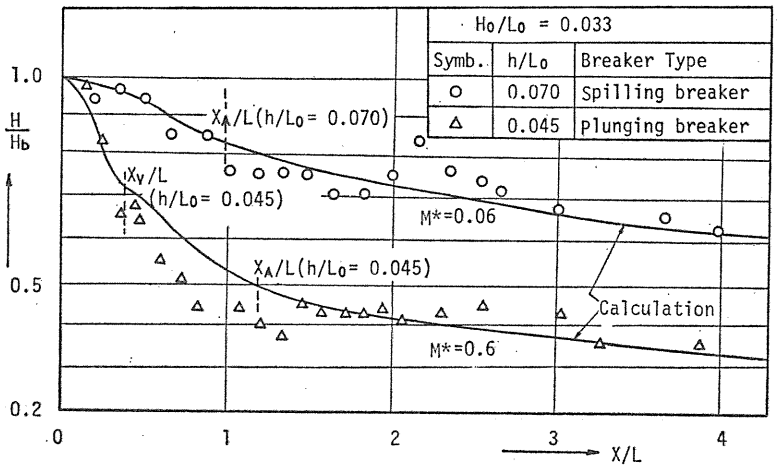

Fig. 32. Comparison of calculated values with experimental values.

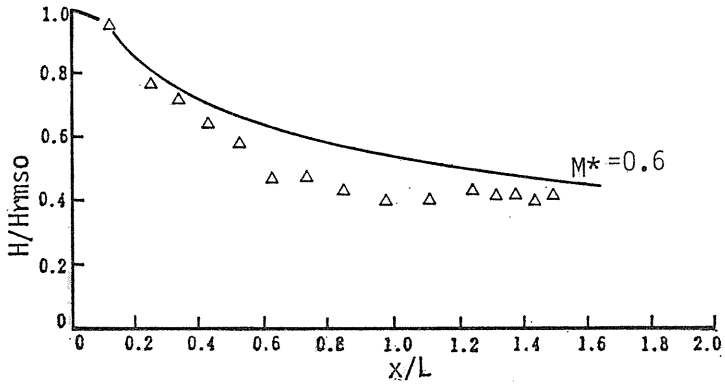

Fig. 33. Comparison between fields measurements and calculated values (from Suhayda[53]).

6. 5. Energy method

6. 5. 1. Battjes' model

The treatment of wave height attenuation by means of the energy method have been performed by many researchrs, e. g., Le méhauté,[42] Horikawa and Kuo,[40] Battjes,[31] etc,. Horikawa and Kuo calculated, as mentioned already, the wave height decay by assuming the breaker-caused turbulence as the isotropic turbulence as well as by using a solitary wave. On the other hand, Battjes[31] used the concept of a bore like Le méhauté. Battjes applied it to the wave height decay of a random wave, and he proposed a method to calculate the wave height variation and the mean water level variation. He used the equation of energy balance given by

$$\frac{\partial(EC_g)}{\partial x}+D=0, \tag{65}$$

where, E is the wave energy per unit area, C_g is the group velocity, and D is the power dissipated.

The problem is the estimation of D. By using the assumption that broken waves satisfy the relation of $H/h\fallingdotseq 1$, and introducing the probability of wave breaking Q_b (at a fixed point), Battjes derived D from Eq. (21),

$$D=\frac{\alpha}{4}Q_b\bar{f}\rho g H_m^2, \tag{66}$$

where, α is a numerical constant, $\bar{f}$ is the mean frequency of wave power spectrum, and H_m is the critical wave height. Battjes used the wave height distribution given by,

$$\begin{aligned} F(H)&=1-\exp\left(-\frac{1}{2}H^2/\hat{H}^2\right), && 0\leqq H<H_m \\ &=1, && H_m\geq H \end{aligned} \tag{67}$$

where, $\hat{H}$ is the modal value. H_m, H_{rms} (rms value of wave height H) and Q_b

satisfy the following two relations,

$$H_{rms}^2=\int_0^\infty H^2 dF(H)=2(1-Q_b)\hat{H}^2, \tag{68}$$

$$Q_b=\exp\left(-\frac{1}{2}H_m^2/\hat{H}^2\right). \tag{69}$$

From Eqs. (68) and (69),

$$\frac{1-Q_b}{\ln Q_b}=-\left(\frac{H_{rms}}{H_m}\right)^2. \tag{70}$$

where, E and C_g in Eq. (65) are given by

$$E=\frac{1}{8}\rho g H_{rms}^2, \tag{71}$$

$$C_g=\left[\frac{2\pi f}{k}\left(\frac{1}{2}+\frac{k(h+\eta)}{\sinh 2k(h+\eta)}\right)\right]_{f=\bar{f}}. \tag{72}$$

The mean water level η is calculated by the following realtion,[54]

$$\frac{d\eta}{dx}=-\frac{1}{(\eta+h)}\frac{d}{dx}\left[\frac{1}{8}\overline{H^2}\left(\frac{1}{2}+\frac{2kh}{\sinh 2kh}\right)\right]. \tag{73}$$

The variation of H_m after wave breaking can be estimated by Eqs. (65), (66), and (70) with help of Eqs. (71), (72) and (73). In Eqs. (72) and (73), k is the wave number ($=2\pi/L$).

Figs. 34 and 35 show comparisons between calculated values and experiments on a uniform slope bed and on a sloping beach with sand bar, respectively. In these figures, H_{rmso} indicates value of H_{rms} in deep water. The coefficients, α and γ are decided in order that the calculations may agree with experiments. It should be noted that $Q_b=1$ in Eq. (66) corresponds to the case of the regular wave.

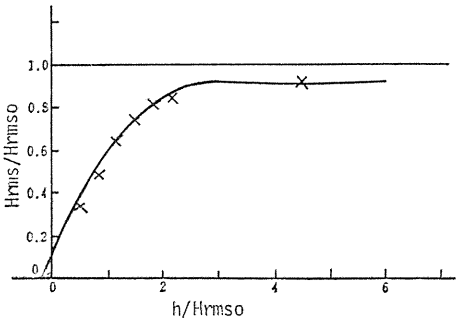

Fig. 34. Comparison between calculated values and experimental values (from Battjes[31]).

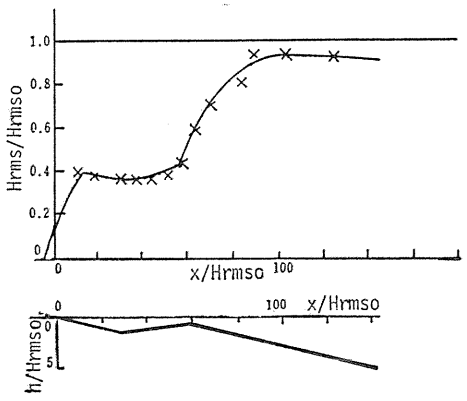

Fig. 35. Comparison between calculated values and experiments (from Battjes[31]).

5. 6. 2. Authors' model

In order to predict the variation of wave height and period due to shoaling and breaking, some theoretical treatments have been proposed.[29, 31, 34, 55~57] Each theoretical treatment has its merit and demerit. In this paper, the theoretical treatment proposed by the present authors is introduced.

6. 5. 2. 1. Joint probability density function of wave in deep water

The joint probability density function of wave height and period P_r (H, T) is assumed here to be the simple product of the wave height distribution P_r (H) and the wave period distribution $P_r(T)$. $P_r(H)$ and $P_r(T)$ are assumed to be Rayleigh distribution and T^2-Rayleigh distribution, respectively.

$$P_r(H,\ T)=P_r(H)P_r(T), \tag{74}$$

$$P_r(H)=\frac{\pi}{2}\frac{H}{\overline{H}^2}\exp\left[-\frac{\pi}{4}\left(\frac{H}{\overline{H}}\right)^2\right], \tag{75}$$

$$P_r(T)=2.7\frac{T^3}{\overline{T}^4}\exp\left[-0.675\left(\frac{T}{\overline{T}}\right)^4\right]. \tag{76}$$

where, $\overline{H}$ and $\overline{T}$ are the mean wave height and period, respectively.

6. 5. 2. 2. Breaking condition

The breaking condition presented by Goda for the regular wave is used for the first approximation.

$$\frac{H_b}{h_b}=0.17(h_b/L_o)^{-1}[1-\exp(1.5\pi(h_b/L_o)(1-15\tan\theta^{4/3}))] \tag{77}$$

6. 5. 2. 3. Shoaling condition

The shoaling condition for the small amplitude wave of the regular wave is used in the calculation.

$$H_s=K_sH_o, \tag{78}$$

$$K_s=[\tanh k(h+\bar{\eta})+k(h+\bar{\eta})(1-\tanh^2 k(h+\bar{\eta}))] \tag{79}$$

where, K_s is the shoaling factor, H_o is the wave height in deep water, H_s is the wave height at the depth of h, $k=2\pi/L$, and $\bar{\eta}$ is the mean water level.

6. 5. 2. 4. Variation of mean water level

The mean water level $\bar{\eta}$ at the depth of h is calculated by the following equation (Longuet-Higgins and Stewart[54]).

$$\frac{d\bar{\eta}}{dx}=-\frac{1}{(\bar{\eta}+h)}\frac{d}{dx}\left[\frac{1}{8}\overline{H}^2\left(\frac{1}{2}+\frac{2kh}{\sinh 2kh}\right)\right]. \tag{80}$$

In calculating the equation (80), the following difference form is used,

$$\bar{\eta}_{i+1}=\bar{\eta}_i-\frac{D_k}{(h+\bar{\eta})_{i+1/2}}[\overline{H^2}_{i+1}-\overline{H^2}_i], \tag{81}$$

where,

$$(h+\bar{\eta})_{i+1/2}=\frac{1}{2}((h+\bar{\eta})_i+(h+\bar{\eta})_{i+1}), \tag{82}$$

$$D_k=\frac{1}{8}\left[\frac{1}{2}+\frac{2kh}{\sinh 2kh}\right]. \tag{83}$$

In Eqs. (79)$\sim$(82), $\overline{H^2}$ is the mean square wave height, subsuffix i and $i+1$ are locations of calculation, and x is the horizontal distance.

6. 5. 2. 5. Re-distribution of breaking waves

Individual waves of which H/h is larger than those given by Eq. (77) break and are transformed to smaller waves. Therefore, the joint probability density corresponding to breaking waves (the shadow area in Fig. 36 (b)) should be re-distributed to the rest portion. The probability density of the breaking waves is

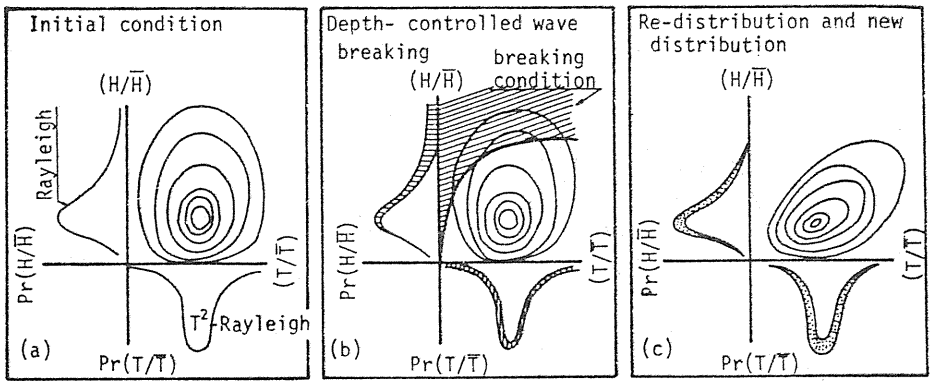

Fig. 36. Schematic illustration of variation of joint probability density of wave heights and periods due to wave breaking.

assumed here to be re-distributed proportional to the probability density of the rest non-breaking wave. The dotted portion of the wave height and period distribution in Fig. 36 (c) indicates the probability density which is added. Then, in this way, a new probability density of the irregular wave is determined as shown in the first quadrant in Fig. 36 (c).

6. 5. 2. 6. Procedure of calculation

The calculation starts from the deep water condition $h/L_o=1.0$ and with the initial joint probability density of wave given by Eqs. (74), (75) and (76). In the calculation, the stillwater depth on a sloping beach is devided into many portions, i. e., the divided non-dimensional stillwater depth $\Delta h/H_o$ is 100, 10, 1, 0. 25, and 0. 05 for $h/H_o\geq 100$, $20\leq h/H_o<100$, $5\leq h/H_o<20$, $2\leq h/H_o<5$, $0\leq h/H_o<2$, respectively.

The joint probability density is, also, divided into 14400 meshes to calculate the change of the joint probability density due to shoaling and breaking.

The shoaling factor K_s at the location $(i+1)$ is first calculated by the known values of $\overline{T}$ and $\overline{\eta}$ at the location (i). The modified joint probability density due to shoaling at the location $(i+1)$ is calculated by the known joint probability density at the location (i) and the shoaling factor at the location $(i+1)$. Next, the modified joint probability density at the location $(i+1)$ is modified again by the wave breaking condition of Eq. (77). The probability density corresponding to breaking waves is re-distributed to the non-breaking wave portion, as mentioned at *6. 5. 2. 6.* Therefore, the new joint probability density function at the location $(i+1)$ is determined. The mean water level $\overline{\eta}$ at the location $(i+1)$ is calculated from Eqs. (81), (82) and (83). In the calculation, the stillwater depth h is replaced by $h+\overline{\eta}$ in determing wave characteristics.

6. 5. 2. 7. Calculated values and discussions

The change of non-dimensional wave height $H_{1/3}/H_o$ with h/H_o calculatied by the present authors' model is similar to that of Goda's calculation, as in Fig. 37. However, the calculations of the present authors are generally smaller than that of Goda. This is largely attributed to the reason that Goda used the shoaling factor for the finite amplitude wave theory, while the present authors used that for the

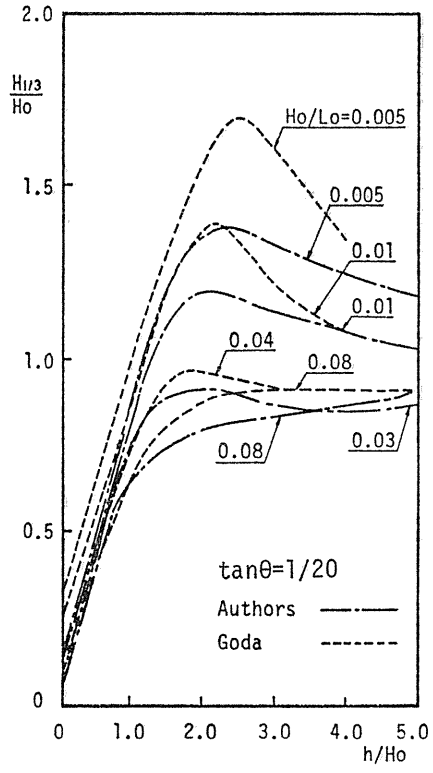

Fig. 37. Calculated values of significant wave height.

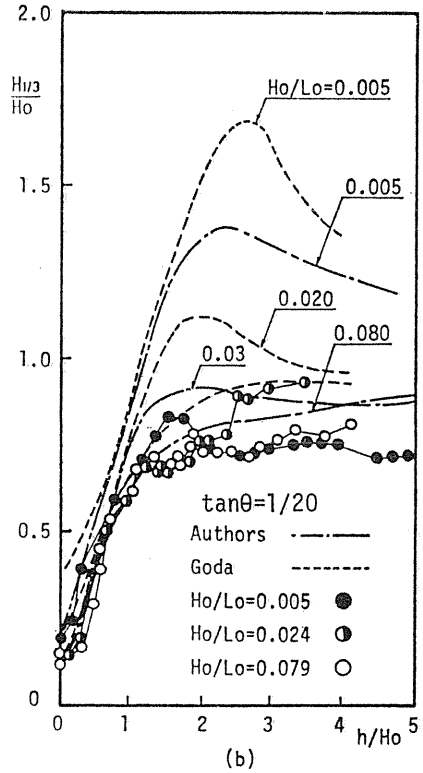

Fig. 38. Comparison between calculated values and experiments.

small amplitude wave theory. The qualitative agreement between calculation and experiments is recognized (see Fig. 38). The difference may be improved by establishing a better breaking criterion and adopting a non-linear wave interaction between individual waves.

The variation of statistical wave periods due to shoaling and breaking has not been discussed so much as that of statistical wave height. Goda[34], and Hotta[58] showed that statistical wave periods such as $\overline{T}$, $T_{1/3}$, and T_{max} become larger as the wave approaches to the shore line. Fig. 39 shows one example of calculation of $T_{1/3}/[T_{1/3}]_o$ with h/H_o, where $[T_{1/3}]_o$ is the significant wave period in deep water condition. Although the numerical estimations predict higher values than the experiment, it can be said that experimental trend agrees qualitatively well with calculations.

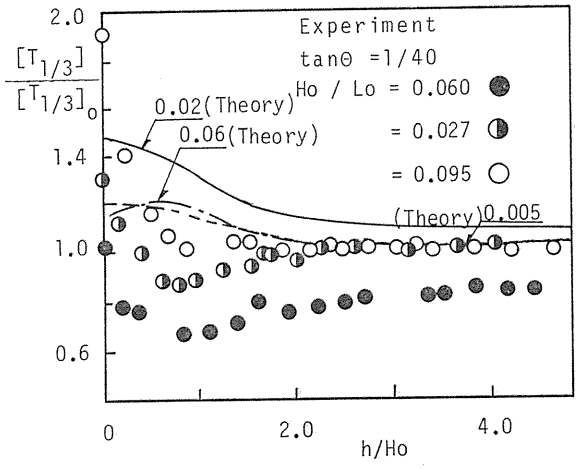

Fig. 39. Comparison between calculated values and experiments.

7. Wave run-up height

7. 1. Regular wave

The final stage of the wave transformation after wave breaking is the phenomenon of wave run-up on a dry bed. The wave run-up height is a very important factor in determining the construction location of seawalls, the design height of beach nourishment works, the sand drift zone for prediction of the change of beach profile, etc..

The theoretical considerations on the wave run-up height have been performed by many researchers since Stoker solved the non-linear shallow water wave theory by means of the characteristics method. In particular, the achievement of Freeman and Le Méhauté[59] on the run-up mechanism of solitary wave on a dry bed gave a significant suggestion to the run-up problem of periodic waves on a dry bed. Some researchers, however, doubt the application of the above-mentioned treatments using the solitary wave or a bore to the run-up phenomenon of the periodic waves.

This is due to the reason that the run-up of the periodic waves largely depends upon the back-wash of a preceeding wave as well as the water depth at the wave front, so the resulting run-up mechanism is more complicated. Therefore, emperical formulas based on laboratory experiments have been presented to predict the wave run-up heigh. Among them, Hunt's empirical formula[60] is popular because it is comparatively easy to use,

$$\frac{R}{H_b}=c_p\frac{\tan\theta}{(H_b/L_o)^{1/2}}, \tag{84}$$

where, R is the run-up height from the stillwater level, c_p is a numerical constant relating to the permeability of bottom and $c_p=1$ for the impermeable bottom and $c_p<1$ for a permeable bottom, H_b is the wave height at breaking point, L_o is the wave length in deep water, and $\tan\theta$ is the bottom slope.

The present authors[61] found out, in their experiments, that the stillwater depth h_o at the toe of the bottom slope plays an important part on the run-up height, and they proposed the following equation,

$$\begin{aligned}&\frac{R}{H_o}=P(\tan\theta)\left(\frac{H_o}{L_o}\right)^{-1/2}(h_o/L_o)^{Q(\tan\theta)},\\&P(\tan\theta)=4.56\times10^{-2}(\tan\theta)^{-0.133},\\&Q(\tan\theta)=-0.421\ ;\ \text{for}\ \tan\theta=1/5,\\&\qquad=5.85\times10^{-3}(\tan\theta)^{-1.246}\ ;\ \text{for}\ 1/40\leq\tan\theta\leq1/10.\end{aligned} \tag{85}$$

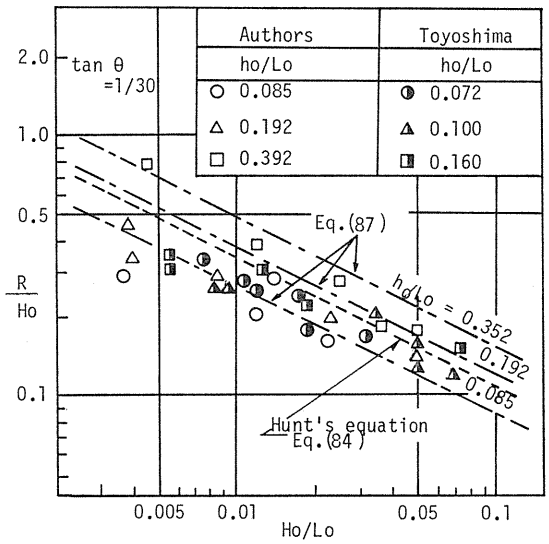

Fig. 40. Effect of h_o/L_0 to R/H_o.

It should be noted that Eq. (85) is valid for $\tan\theta\leq1/5$. Fig. 40 shows a comparison among calculated values of Eqs. (84) and (85), and experimental values

obtained by the present authors and by Toyoshima et al.[62]. The run-up height predicted by Eqs. (84) and (85) decreases as the bottom slope becomes gentler. However, in case of steep slopes ($\tan\theta \geq 1/5$) like those of breakwaters or sea-dikes, the run-up height tends to become higher with decreasing the bottom slope. Fig. 41 shows experimental results on uniform bottom slopes performed by Savage[63], and the above-cited fact for the bottom slope effect to the run-up height is clearly seen.

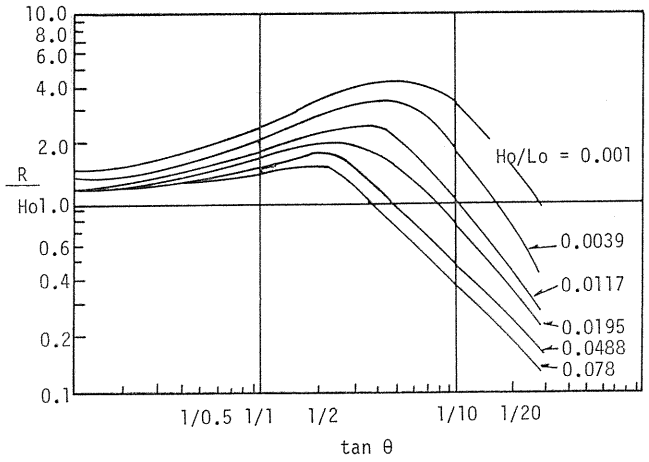

Fig. 41. Relation between R/H_o and $\tan\theta$ (from Savage[63]).

7. 2. *Irregular wave*

It may be one of the interesting points to study the possibility of extending the empirical formulas deduced for the regular wave to the run-up height problems of the irregular wave. One interesting problem is whether the significant wave run-up height $R_{1/3}$ of the irregular wave can be equal to the run-up height of the regular wave corresponding to the significant wave or not.

Fig. 42 shows a relation between the ratio $(R_{1/3}/H_{o1/3})_{IR}/(R/H_o)_{RE}$ and the bottom slope, where $(R_{1/3}/H_{o1/3})_{IR}$ indicates a relative significant run-up height in irregular wave and $(R/H_o)_{RE}$ is a relative run-up height estimated by Eq. (85) for regular waves. In Fig. 42, h_o is the stillwater depth at the toe of bottom slope, $L_{o1/3}$ and $H_{o1/3}$ are the significant wave length and height in deep water. As seen from Fig. 42, the relative significant run-up height $(R_{1/3}/H_{o1/3})_{IR}$ almost correponds to the relative run-up height $(R/H_o)_{RE}$ of regular waves for $\tan\theta \geq 1/10$. But, in case of $\tan\theta \leq 1/15$, $(R_{1/3}/H_{o1/3})_{IR}$ becomes smaller than $(R/H_o)_{RE}$. The reason is not well explained at present because the mechanism of wave run-up has not been revealed from the hydrodynamic point of view. However, it will be guessed that run-ups of larger waves among individual waves are predominant and they have a strong effect to the run-up of smaller waves, in case of the irregular wave.

Now, let us discuss a distribution of run-up height for the irregular wave. Battjes[64] derived an expression for the probability distribution of wave run-up

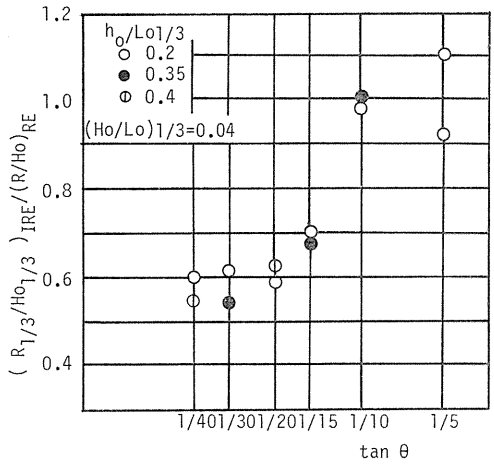

Fig. 42. Comparison between run-up heights of irregular wave and regular wave.

height. His theoretical development was, however, largely supported by the assumptions; (1) run-up of individual waves in an irregular wave train indicates the value following Hunt's and (2) the joint porbability distribution of wave heights and periods can be expressed by the bivariate Rayleigh distribution. But, as pointed out by Iwagaki[65], the wave period is not T^2-Rayleigh distributed. Its distribution depends upon a wave spectral shape, then a Weibull distribution will be a more general expression form. Then, the present authors used the Weibull distribution for the joint probability density function of wave heights and periods. The joint probability function $P(H, T)$ expressed by a bivariate Weibull probability density is given by

$$\begin{aligned} P(H, T) &= P(H)P(T), \\ &= A_H m_H (H/H_r)^{m_H-1} \exp[-A_H (H/H_r)^{m_H}]\left(\frac{1}{H_r}\right) \\ &\times A_T m_T (T/T_r)^{m_T-1} \exp[-A_T (T/T_r)^{m_T}]\left(\frac{1}{T_r}\right), \end{aligned} \tag{86}$$

where, the variables of H and T are treated here as statistically independent, and m_H and m_T are the shape factors of the Weibull probability density function of wave heights and periods, respectively, A_H and A_T are the scale factors of the Weibull probability density function of wave heights and periods respectively, and H_r and T_r are the mean square values of wave heights and periods, respectively. The present authors assumed the followings;

(1) the run-up height of individual waves in the irregular wave train is given by Eq. (85),

and

(2) the wave height distribution is Rayleigh distribution, i. e., $m_H=2.0$ and $A_H=1.0$.

Using the assumptions, the present authors proposed Eq. (87) to estimate the

distribution of wave run-up height in the irregular wave.

$$F(r^*)=\int_0^{r^*} f(r^*)\,dr^*, \tag{87}$$

where,

$$\left.\begin{aligned}
&f(r^*)=K_1(r^*)\int_0^{\infty} k_2(t^*)\,dt^*,\\
&k_1(r^*)=t^{*\alpha_1}\exp(\alpha_2),\\
&\alpha_1=m_T-1-8b(\tan\theta),\\
&\alpha_2=-t^{*8b(\tan\theta)}r^{*4}-A_T t^{*m_T},\\
&A_T=\Gamma\left(\frac{m_T+2}{m_T}\right)^{m_T/2},\\
&b(\tan\theta)=0.5-Q(\tan\theta),\\
&Q(\tan\theta)=-0.421,\quad(\tan\theta=1/5),\\
&\qquad=5.85\times10^{-3}\times(\tan\theta)^{-1.246},\quad(1/40\leq\tan\theta<1/5),\\
&r^*=\frac{R}{a(\tan\theta)H_{or}^{1/2}T^{b(\tan\theta)}},\\
&a(\tan\theta)=P(\tan\theta)h_o^{Q(\tan\theta)}(g/2\pi)^{b(\tan\theta)},\\
&P(\tan\theta)=4.56\times10^{-2}\times(\tan\theta)^{-0.133}.
\end{aligned}\right\} \tag{88}$$

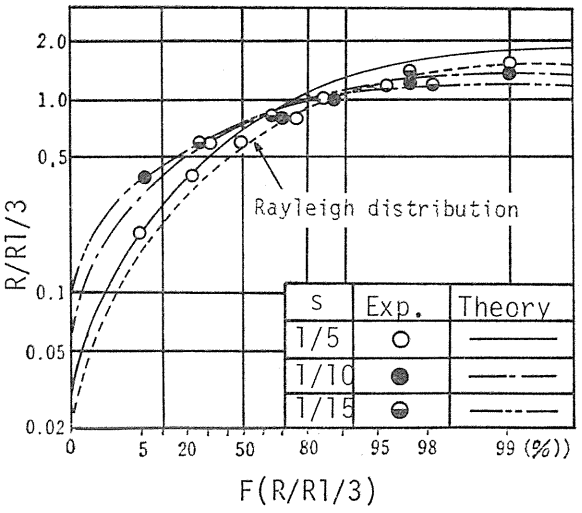

Fig. 43. Distribution of wave run-up height.

In Eq. (88), t^* is the non-dimensional time, Γ is the Gamma function, and H_{or} is the root mean square wave height in deep water.

The probability distribution of the non-dimensional run-up height $R/R_{1/3}$ calculated by Eqs. (87) and (88) is indicated in Fig. 43. The dotted line shows the probability distribution calculated in the case that the distribution of wave heights and periods squared are Rayleigh distributed. The experimental results correspond well to the curves calculated by Eqs. (87) and (88).

8. Concluding remarks

In this paper, the wave characteristics at breaking point and the wave deformation after breaking up to the dry bed are described from theories and experiments, centering on the authors' researches. The wave breaking conditions and breaker types, wave characteristics such as the wave height, wave profiles, etc. at breaking point are described in Section *2*, *3*, and *4*. Next, the internal mechanics of breaking wave are discussed in relation with the horizontal roller, bottom friction, and the turbulence caused by wave breaking, in Section *5* and *6*. And, the quantitative contribution of the roller, bottom friction and the turbulence to the wave energy dissipation in the surf are clarified. Also, in Section *5* and *6*, several new ideas proposed by the present authors are shown, and a new fundamental equation for breaking wave is presentd and its correspondence with experiments is shown to be fairly good. Section *7* showed that the theoretical model for the wave run-up height proposed by the present authors predicts well the experimental facts.

As stated above, a lot of knowledges on wave deformation in the surf zone have been piling up and usefull theoretical treatments and experimental facts are using for practical purposes. However, there are still many problems left to be solved from theories and experiments.

Concerning the regular wave treatment, it is said that theories can predict well the wave height variation in the surf for a moderate value of the so-called turbulence coefficient caused by wave breaking. However, the formulation of the turbulence has not been settled. Detailed experimental investigations on wave kinematics will be needed to improve the theoretical treatment and to establish the basic equation with the turbulence term for the wave in the surf.

On the other hand, in predicting changes of wave heights and periods of irregular waves, the formulation of irregular wave breaking limit is very important. The breaking phenomenon of the irregular wave is very different from that of the regular wave[66]. Therefore, as far as the breaking limit of the regular wave is adopted as an approximation, it should be noted that a quantitative agreement between theoretical models and experiments will not be obtained.

References

1) Iversen, H. W.: Laboratory study of breakers, Gravity waves, N. B. S., Circular 521, 1951, 9-32.
2) Rankine, W. J.: Summary of properties of certain stream lines, Phil. Mag. (4) 29,

1864, 282-288.
3) Boussinesq, J.: Theorie de l'intumescence liguide appelee onde solitaire ou de translation se propagent dans un canal rectangulaire, Institute de France, Academi de Sciences, Comptes Rendus, June 9, 1871.
4) McCowan, M. A.: On the heighest wave of permenent type, Phil. Mag. S5, Vol. 38, No. 233, Oct. 1894, 351-358.
5) Munk, W. H.: The solitary wave and its application to surf problem, Ann. N. Y. Acad. Sci., 51, 1949, 376-424.
6) Miche, A.: Mouvements ondulatories de la mer en profondeur constante ou decroissante. Forme limit de la houle lors de som deferlement: Application aux digues maritimes. Ann. Ponts et Chausse, Tom 114, 1944.
7) Hamada, T.: Breakers and beach erosion: Rept. Trans. Tech. Res., Inst., Rept. No. 1, 1951.
8) Sato, S.: Surf waves in shallow water, Jour. Res. Public Works. Res. Inst., Vol. 1, 1954 (in Japanese).
9) Kishi, T.: Study on breakwaters (4), breaking limit of progessive wave: Rept. Res. Public Works, Res. Inst., Vol. 1, 1954 (in Japanese).
10) Stokes, G. G.: On the change of oscillatory waves, Trans. of the Cambridge Phil. Soc., Vol. 8, 1847, 314.
11) Greenspan, H. G.: On the breaking of waver waves of finite amplitude on a sloping beach, Jour. Fluid. Mech., No. 4, 1958, 330-334.
12) Kishi, T.: Transformaiton, breaking and run-up of a long wave of finite height. Proc. 8th Conf. on Coastal Eng., 1961, 60-76.
13) Murota, A.: Transformation of surges, Proc. 10th Conf. on Coastal Eng., Vol. 1, 1951, 382-395.
14) Shuto, N.: On the finite amplitude wave—breaking limit of progressive wave by higher order power series solution—, Rept. Res. Public Works. Res. Inst., Vol. Ⅲ, 1961 (in Japanese).
15) Stoker, J. J.: The formation of breakers and bores. The theory of nonlinear wave propagation in shallow water and open channels, Comm. Pure. Appl. Math., Vol. 1, 1948, 1-87.
16) Le Méhauté, B. and R. C. Y. Koh: On the breaking of waves arriving at an angle to the shore, Jour. of Hydraulic Res., 5, Vol. 1, 1967, 67-88.
17) Goda, Y.: Study on design pressure of breakwater, Rept., Port and Harbor Res. Inst., Vol. 12, No. 3, 1973 (in Japanese).
18) Patric, D. A. and R. L. Wiegel: Amphibian tractors in the surf, Proc. 1st Conf. on Ships and waves, 1955, 397-422.
19) Galvin, C. J.: Breaker classification on three laboratory beaches, Jour. Geoph. Res., Vol. 73, No. 12, 1968, 175-200.
20) Hayami, S.: Mechanics of wave breaking (Ⅱ), Proc. 2nd. Japanese Conf. on Coastal Eng., 1954, 13-15 (in Japanese).
21) Battjes, J. A.: Surf similarity parameter, Proc. 14th Conf. on Coastal Eng., 1974, 466-480.
22) Sawaragi, T. and K. Iwata: Fundamental study on mechanics of wave breaking (1), Proc. 16th Japanese Conf. on Coastal Eng., 1969, 35-39 (in Japanese).
23) Wilson, B. W., L. M. Webb and J. A. Hendrickson: The nature of tsunami, their geneartion and dispersion in water of finite depth, NESCO Tech. Rept., No. 57-2, 1946.
24) Hydraulic Mannual: Showa 46-revised edition, Tokyo, JSCE, 1971.
25) Sawaragi, T. and K. Iwata: Experimental studies on irregular wave deformation due to depth-controlled wave breaking, Proc. Inter. Symp. on Hydrodynamics in Ocean Eng., Vol. 1, 1981, 166-182.
26) Weishar, L. L. and R. J. Byrne: Field study of breaking wave characteristics, Proc. 16th Conf. on Coastal Eng., 1978, 486-506.

27) Goda, Y.: On arrangement of breaker index, Proc. JSCE, Vol. 180, 1970, 39-50 (in Japanese).
28) Kemp, P. H.: Wave asymmetry in the nearshore zone and breaker area, Near Shore Sediment Dynamics and Sedimentation, J. Haris and A. Carr ed., John Wiley & Sons, 1975.
29) Collins, J. I.: Probabilities of breaking wave characteristics, Proc. 12th Conf. on Coastal Eng., 1970, 399-414.
30) Battjes, J. A.: Set-up due to irregular waves, Proc. 13th Conf. on Coastal Eng., 1972, 143-147.
31) Battjes, J. A. and J. P. F. M. Janssen: Energy loss and set-up due to breaking of random waves, Proc. 16th Conf. on Coastal Eng., 1978, 569-587.
32) Kuo, K. and S. Kou: Wave height decay of breaking wind waves and distribution of wave height, Proc. 19th Japanese Conf. on Coastal Eng., 1972, 137-142 (in Japanese).
33) Nath, J. H. and F. L. Ramsey: Probability distribution of breaking wave heights emphasizing the utilization of the JONSWAP spectrum, Jour. Phys. Oceano., Vol. 6, No. 3, 1976, 316-323.
34) Goda, Y.: Deformation of irregular waves due to depth-controlled wave breaking, Rept., Port and Harbor Res. Inst., Vol. 14, No. 3, 1975 (in Japanese).
35) Iwagaki, Y., A. Kimura and Y. Kishida: Study on the irregular wave breaking on sloping beaches, Proc. 24th Japanese Conf. on Coastal Eng., 1977, 102-106 (in Japanese).
36) Komar, P. D. and Gaughan, M. K.: Airy wave theory and breaker height prediction, Proc. 13th Conf. on Coastal Eng., 1972, 405-418.
37) Sawaragi, T., K. Iwata and N. Matsumoto: Wave deformation after breaking, Proc. 20th Japanese Conf. on Coastal Eng., 1973, 565-570 (in Japanese).
38) Führböter, A.: Air entrainment and energy dissipation in breakers, Proc. 12th Conf. on Coastal Eng., 1970, 391-398.
39) Peregrine, D. H. and I. A. Svendsen: Spilling breakers, bores and hydraulic jumps, Proc. 16th Conf. on Coastal Eng., 1978, 540-550.
40) Horikawa, K. and C. T. Kuo: A study on wave deformation inside surf zone, Proc. 10th Conf. on Coastal Eng., 1966, 217-233.
41) Sawaragi, T. and K. Iwata: On wave deformation after breaking, Proc. 14th Conf. on Coastal Eng., 1974, 481-499.
42) Le Méhauté, B.: On non-saturated breakers and the wave run-up, Proc. 8th Conf. on Coastal Eng., 1963, 77-92.
43) Eagleson, P. S.: Laminar damping of oscillatory waves, Proc. ASCE, Vol. 88, No. HY3, 1962, 155-181.
44) Iwagaki, Y., Y. Tsuchiya and K. Chin: Experimental study on wave attenuation due to bottom friction (3), Proc. 18th Japanese Conf. on Coastal Eng., 1965, 41-49 (in Japanese).
45) Sawaragi, T. and K. Iwata: Wave spectrum of breaking waves, Proc. 15th Conf. on Coastal Eng., 1974, 580-594.
46) Sawaragi, T. and K. Iwata: Wave spectrum changes in shallow water surf, Proc. 26th Japanese Conf. on Coastal Eng., 1979, 105-108. (in Japanese).
47) Phillips, O. M.: The dyanmics of upper ocean, Cambridge University Press, 1966, 43-47.
48) Ijima, T., T. Matsuo, T. and K. Koga: Equilibrium range spectra in shoaling water, Proc. 12th Conf. on Coastal Eng., 1970, 539-556.
49) Kitaigordskii, S. A., Krasitskii, V. P. and M. M. Zaslauskii: On Phillips' theory of equilibrium range in the spectra of wind-generated gravity waves, Jour. Phys. Ocean., Vol. 5, 1975, 410-420.
50) Thornton, E. B.: Rederivation of the saturated range in the frequency spectrum of wind-generated waves, Jour. Phys. Ocean., Vol. 7, 1977, 137-140.
51) Stoker, J. J.: Water waves, Pure and Appl. Math., Vol. Ⅳ, Intersience Pub., INC., New York, 1957, 291-448.

52) Keller, H, B., D. A. Levine and G. B. Whitham: Motion of a bore over a sloping beach, Jour. Fluid Mech., Vol. 7, 1960, 302–316.
53) Suhayda, J. N. and N. R. Pettigrew: Observations of wave height and wave celerity in the surf zone, Jour. Geophy. Res., Vol. 82, No. 9, 1977, 1419–1424.
54) Longuet-Higgins, M. S. and R. W. Stewart: Radiation stresses in water waves, a physical discussion, with application, Deep Sea Res.. Vol. 11, 1964, 529–562.
55) Iwagaki, Y., H. Mase and T. Tanaka: Modeling for irregular wave transformation in surf zone, Proc. 28th Japanese Conf. on Coastal Eng., 1981, 104–108 (in Japaneses).
56) Iwata, K. and H. Fukuyo: Change of zero-up cross spectrum on sloping beaches, Proc. 29th Japanese Conf. on Cosatal Eng., 1982, 60–64 (in Japanese).
57) Sawaragi, T., K. Iwata and T. Azuma: Changes of mean water level due to irregular waves, Proc. 25th Japanese Conf. on Coastal Eog., 1978, 184–187 (in Japanese).
58) Hotta, S. and M. Mizuguchi: Field measurement of wind waves in the surf, Proc. 26th Japanese Conf. on Coastal Eng., 1979, 152–156 (in Japanese).
59) Freeman, J. C. and Le Méhauté, B.: Wave breakers on a beach and surges on a dry bed, Proc. ASCE, HY2, 1964, 187–216.
60) Hunt, I. A. J.: Design of seawalls and breakwaters, Proc. ASCE, Vol. 85, No. WW3, 1957, 123–152.
61) Sawaragi, T., K. Iwata and A. Morino: Wave run-up height on gentle slopes, Coastal Engineering in Japan, JSCE, Vol. 20, 1977, 83–94.
62) Toyoshima, O, N. Shuto and H. Hashimoto: Wave run-up height on sea-dikes-beach slope of 1/30, Proc. 11th Japanese Conf. on Coastal Eng., 1964, 260–265 (in Japanese).
63) Savage, R. R.: Laboratory data on wave run-up on roughened and permeable slopes, Proc. ASCE, WW3, 1958, 1640–1～1640–38.
64) Battjes, J. A.: Run-up distributions of waves breaking on slopes, Proc. ASCE, WW1, 1971, 91–114.
65) Iwagaki, Y. and A. Kimura: Study on probability of wave period of irregular sea waves, Proc. 22nd Japanese Conf. on Coastal Eng., 1975, 295–300 (in Japanese).
66) Iwata, K.: Run-up of irregular wave on slopes, Lecture Notes, 18th Summer Seminar on Hydraulics, Course B, Committee on Hydraulics, JSCE, 1982, 3–1～3–18 (in Japanese).